

Jagged Islands of Bound Entanglement and Witness-Parameterized Probabilities

Paul B. Slater*

Kavli Institute for Theoretical Physics,

University of California,

Santa Barbara, CA 93106-4030

(Dated: June 1, 2020)

arXiv:1905.09228v4 [quant-ph] 29 May 2020

Abstract

We report several witness-parameterized families of bound-entangled probabilities. Two pertain to the $d = 3$ (two-qutrit) and a third to the $d = 4$ (two-ququart) subsets analyzed by Hiesmayr and Löffler of “magic” simplices of Bell states that were introduced by Baumgartner, Hiesmayr and Narnhofer. The Hilbert-Schmidt probabilities of positive-partial-transpose (PPT) states—within which we search for bound-entangled states—are $\frac{8\pi}{27\sqrt{3}} \approx 0.537422$ ($d = 3$) and $\frac{1}{2} + \frac{\log(2-\sqrt{3})}{8\sqrt{3}} \approx 0.404957$ ($d = 4$). We obtain bound-entangled probabilities of $-\frac{4}{9} + \frac{4\pi}{27\sqrt{3}} + \frac{\log(3)}{6} \approx 0.00736862$ and $\frac{-204+7\log(7)+168\sqrt{3}\cos^{-1}(\frac{11}{14})}{1134} \approx 0.00325613$ ($d = 3$) and $\frac{8\log(2)}{27} - \frac{59}{288} \approx 0.00051583$ and $\frac{24\text{csch}^{-1}(\frac{8}{\sqrt{17}})}{17\sqrt{17}} - \frac{91}{544} \approx 0.00218722$ ($d = 4$). (For $d = 3$, we also obtain $\frac{2}{81}(4\sqrt{3}\pi - 21) \approx 0.0189035$ based on the realignment criterion. Thus, the total entanglement probability appears to equal $(1 - \frac{8\pi}{27\sqrt{3}}) + \frac{2}{81}(4\sqrt{3}\pi - 21) = \frac{13}{27} \approx 0.481481$.) The families, encompassing these results, are parameterized using generalized Choi and Jafarizadeh-Behzadi-Akbari witnesses. In the $d = 3$, analyses, we utilized the mutually unbiased bases (MUB) test of Hiesmayr and Löffler, and also the Choi $W^{(+)}$ test. The same bound-entangled probability was achieved with both—the sets (“jagged islands”) detected having void intersection. The entanglement (bound and “non-bound”/“free”) probability for both was $\frac{1}{6} \approx 0.16667$, while their union and intersection gave $\frac{2}{9} \approx 0.22222$ and $\frac{1}{9} \approx 0.11111$. Further, we examine generalized Horodecki states, as well as estimating PPT-probabilities of approximately 0.39339 (very well-fitted by $\frac{7\pi}{25\sqrt{5}} \approx 0.39338962$) and 0.115732 (conjecturally, $\frac{1}{8} + \frac{\log(3-\sqrt{5})}{13\sqrt{5}} \approx 0.115737$) for the original (8- [two-qutrit] and 15 [two-ququart]-dimensional) magic simplices themselves.

PACS numbers: Valid PACS 03.67.Mn, 02.50.Cw, 02.40.Ft, 02.10.Yn, 03.65.-w

*Electronic address: slater@kitp.ucsb.edu

I. INTRODUCTION

In their landmark 1998 paper, “Volume of the set of separable states”, Życzkowski, Horodecki, Sanpera and Lewenstein stated: “As it was mentioned in the introduction for $N \geq 8$ there are states which are inseparable but have positive partial transposition. Moreover, it has been recently shown that all states of such type represent ‘bound’ entanglement in the sense that they cannot be distilled to the singlet form. The immediate question that arises is how frequently such peculiar states appear in the set of all the states of a given composite system. This question is related to the role of time reversal in the context of entanglement of mixed states....we provide a qualitative argument that the volume of the set of those states is also nonzero” [1, sec. V].

We will here offer some *quantitative* arguments in this direction (cf. [2]), where the sets of primary interest are the “magic” simplices of Bell states (sec. II) [3–6]—for which it had been noted that the “Hilbert-Schmidt metric defines a natural metric on the space state” [3]—and generalized Horodecki states (sec. IV) [7, 8].

II. MAGIC SIMPLICES ANALYSES

Within the magic simplex setting of Baumgartner, Hiesmayr and Narnhofer [3, 4], the case of bound entanglement of two photonic qutrits using the orbital angular momentum degree of freedom of light was investigated in a 2013 paper of B. C. Hiesmayr and W. Löffler [9]. They noted that this was the simplest case of bound entanglement, with “complications, such as those arising in multipartite systems, not occurring”.

Their equation (7) for a density matrix ρ_d in the $(d^2 - 1)$ -dimensional simplices ($d = 3, 4$) took the form,

$$\rho_d = \frac{q_4(1 - \delta(d - 3)) \sum_{z=2}^{d-2} \left(\sum_{i=0}^{d-1} P_{i,z} \right)}{d} + \frac{q_2 \sum_{i=1}^{d-1} P_{i,0}}{(d-1)(d+1)} + \frac{q_3 \sum_{i=0}^{d-1} P_{i,1}}{d} + \quad (1)$$

$$\frac{\left(-\frac{q_1}{d^2-d-1} - \frac{q_2}{d+1} - (d-3)q_4 - q_3 + 1 \right) \text{IdentityMatrix}[d^2]}{d^2} + \frac{q_1 P_{0,0}}{d^2 - d - 1},$$

the $P_{i,j}$ ’s being orthonormal Bell states. (No explicit ranges were given for the q ’s, and our initial analyses assumed that they would have to be nonnegative. But, it, then, seemed somewhat puzzling that a main example of Hiesmayr and Löffler employed negative q ’s. Also,

we observed that bound entanglement did not seem possible with strictly nonnegative q 's. Eventually, we arrived at the clearly powerful change-of-variables approach—to be shortly detailed—greatly facilitating the exact integrations we had been attempting.)

“This family also includes for $d = 3$ the one-parameter Horodecki-state, the first found bound entangled state. Namely, for $q_1 = \frac{30-5\lambda}{21}$, $q_2 = -\frac{8\lambda}{21}$, $q_3 = \frac{5-2\lambda}{7}$ with $\lambda \in [0, 5]$. This state is PPT for $\lambda \in [1, 4]$ and was shown to be bound entangled for $\lambda \in \{3, 4\}$ [9]. Let us note now—as a prototypical example of our subsequent more demanding three- and four-parameter calculations—that the Hilbert-Schmidt PPT-probability for this one-parameter (λ) Horodecki-state is $\frac{3}{5}$, the probability of entanglement is also $\frac{3}{5}$, and the bound-entangled probability, $\frac{1}{5}$ (cf. [7], and sec. IV below).

A. Transformation between magic simplex parameters, and associated constraints

In the $d = 3$ (two-qutrit) framework, we transform between the nine nonnegative parameters ($c[k, l] \geq 0$, with $k, l = 0, \dots, 2$), summing to 1, employed for the full/original magic simplex of Baumgartner, Hiesmayr and Narnhofer [4, sec. 4], and the three (q_1, q_2, q_3) of the Hiesmayr-Löffler subset. To do so, we use the three equations,

$$c[0, 0] = \frac{1}{180}(32q_1 - 5q_2 - 20q_3 + 20) \equiv Q_1, \quad (2)$$

and

$$c[k, l] = \frac{1}{180}(-4q_1 - 5q_2 + 40q_3 + 20) \equiv Q_2 \quad (3)$$

for $\{k, l\} = \{0, 1\}, \{0, 2\}, \{1, 1\}, \{1, 2\}, \{2, 1\}, \{2, 2\}$, and

$$c[k, l] = \frac{1}{360}(-8q_1 + 35q_2 - 40q_3 + 40) \equiv Q_3 \quad (4)$$

for $\{k, l\} = \{1, 0\}, \{2, 0\}$. (For the indicated Horodecki-state, we have $\{Q_1, Q_2, Q_3\} = \left\{-\frac{2\lambda}{189} + \frac{2}{9\lambda} + \frac{2}{7}, \frac{1}{189}(-11\lambda + \frac{42}{\lambda} + 45), \frac{\lambda^2-21}{27\lambda}\right\}$.)

If we, then, employ Q_1, Q_2 and Q_3 as our principal variables, rather than q_1, q_2, q_3 , using the linear transformations,

$$\{q_1, q_2, q_3\} = \left\{ \frac{5}{3}(4Q_1 + 3Q_2 + 2Q_3 - 1), \frac{8}{3}(Q_1 + 3Q_2 + 5Q_3 - 1), Q_1 + 6Q_2 + 2Q_3 - 1 \right\}, \quad (5)$$

our ensuing analyses simplify greatly. For example, the requirement that ρ_3 is a nonnegative definite density matrix—ensured by requiring that its nine leading nested minors all be

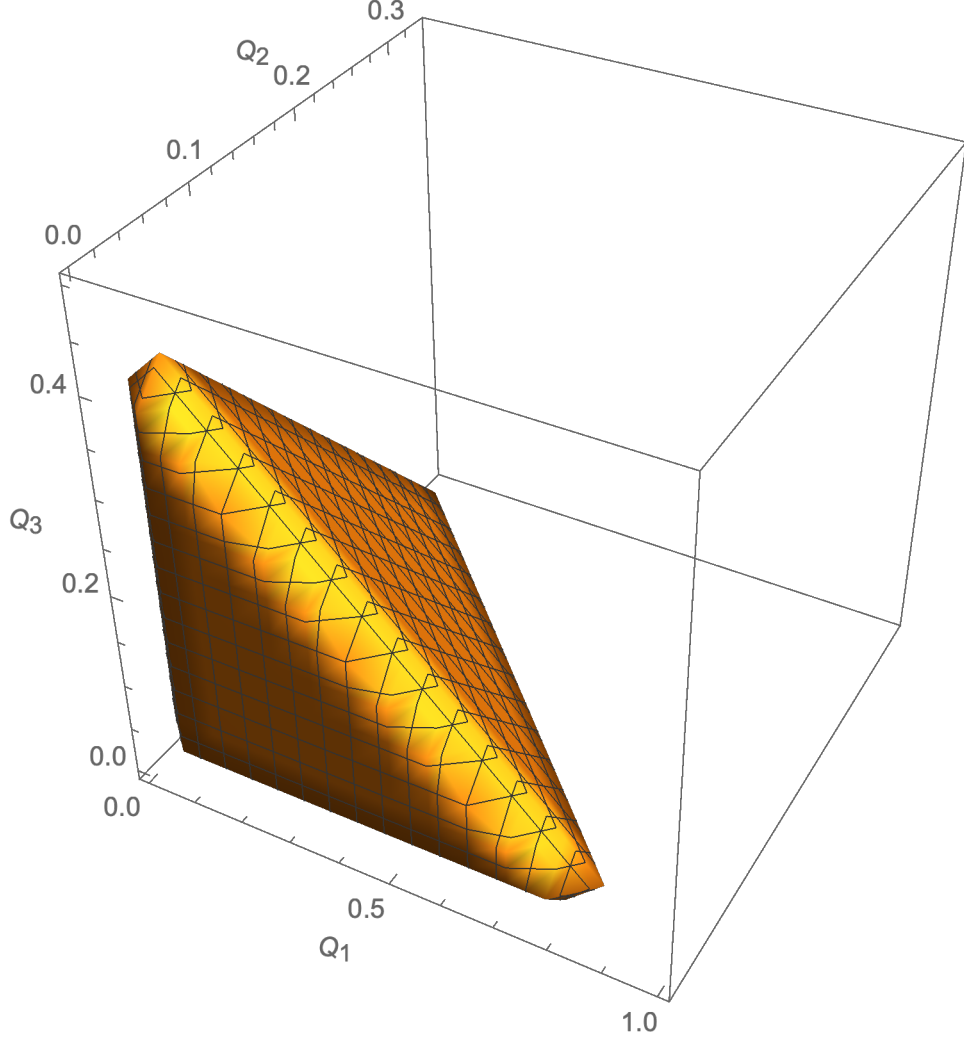


FIG. 1: Convex set of Hiesmayr-Löffler two-qutrit $d = 3$ magic simplex density matrices ρ_3

nonnegative—is transformed from

$$4q_1 + 5q_2 < 40q_3 + 20 \wedge 10q_3 < 4q_1 + 5q_2 + 10 \wedge 4q_1 + 5q_2 + 20q_3 < 20$$

$$\wedge 5(q_2 + 4q_3 - 4) < 32q_1 \wedge (8q_1 - 5(7q_2 - 8q_3 + 8))(8q_1 + q_2 - 8q_3 + 8) < 0$$

to

$$Q_1 > 0 \wedge Q_2 > 0 \wedge Q_3 > 0 \wedge Q_1 + 3Q_2 + 2Q_3 < 1. \quad (6)$$

In Fig. 1 we show the convex set of possible ρ_3 's, in terms of this parameterization. Additionally, the constraint that the partial transpose of ρ_3 is nonnegative definite becomes

$$Q_1 > 0 \wedge Q_3 > 0 \wedge Q_1 + 3Q_2 + 2Q_3 < 1 \wedge Q_1^2 + 3Q_2Q_1 + (3Q_2 + Q_3)^2 < 3Q_2 + 2Q_1Q_3. \quad (7)$$

(We report and employ the $d = 4$ [two-ququart] analogues of the results (2)-(7) in sec. II C.)

1. *MUB test*

Further, the Hiesmayr-Löffler mutually-unbiased-bases (MUB) criterion for bound entanglement, $I_4 = \sum_{k=1}^4 C_{A_k, B_k} > 2$, where C_{A_k, B_k} are correlation functions for observables A_k, B_k [9, Fig. 1] takes the form

$$Q_1 > 3Q_2 + 4Q_3, \quad (8)$$

or, in terms of the original magic simplex parameters

$$3c[0, 0] + c[0, 1] + 2c[0, 2] + c[1, 1] + 2c[1, 2] + c[2, 1] + 2c[2, 2] > 2. \quad (9)$$

2. *Choi test*

Also, Example 2 in [10] states that the ‘‘Choi EW $W^{(+)}$ obtained from the Choi map in $d = 3 \dots$ is given by

$$W^{(+)} = \frac{1}{6} \left(\sum_{i=0}^2 [2|ii\rangle\langle ii| + |i, i-1\rangle\langle i, i-1|] - 3P_+ \right),$$

where $P_+ = |\phi^+\rangle\langle\phi^+|$ with the Bell state $|\phi^+\rangle = (|00\rangle + |11\rangle + |22\rangle)/\sqrt{3}$.’’ It was noted there that this witness (zeros are denoted by dots)

$$W^{(+)} = \frac{1}{6} \begin{pmatrix} 1 & \dots & \dots & -1 & \dots & \dots & \dots & -1 \\ \dots & \dots \\ \dots & \dots & 1 & \dots & \dots & \dots & \dots & \dots \\ \hline \dots & \dots & \dots & 1 & \dots & \dots & \dots & \dots \\ -1 & \dots & \dots & \dots & 1 & \dots & \dots & -1 \\ \dots & \dots \\ \hline \dots & \dots \\ \dots & \dots & \dots & \dots & \dots & \dots & 1 & \dots \\ -1 & \dots & \dots & \dots & -1 & \dots & \dots & 1 \end{pmatrix}, \quad (10)$$

is applicable in the two-qutrit setting. (A related operator $W^{(-)}$ is presented in [10], but it is decomposable and, thus, not capable of detecting bound entanglement. Further, in our particular analysis here, no entanglement at all was detected with its use.) In the Hiesmayr-Löffler $d = 3$ two-qutrit density-matrix setting (1), the entanglement requirement

that $\text{Tr}[W\rho_3] < 0$ takes the simple form

$$2Q_3 + 1 - 2Q_1 - 3Q_2 < 0, \quad (11)$$

or, in terms of the original magic simplex parameters,

$$1/6(-c[0, 0] + c[0, 2] + 2c[1, 0] + c[1, 2] + 2c[2, 0] + c[2, 2]) < 0. \quad (12)$$

B. Two-qutrit analyses ($d = 3$)

In Table I, we report certain computations based on the preceding constraints. Hopefully, these provide insight into the underlying (Hilbert-Schmidt) geometry of the Hiesmayr-Löffler $d = 3$ magic simplex model.

To begin, we obtained findings (Fig. 2, cf. [11]) for the $d = 3$ two-qutrit Hiesmayr-Löffler model that the PPT-probability is $\frac{8\pi}{27\sqrt{3}} \approx 0.537422$, and that the entanglement probabilities revealed by the MUB and Choi tests are both $\frac{1}{6} \approx 0.16667$.

Further, the MUB and Choi bound-entangled probabilities were each determined to equal $-\frac{4}{9} + \frac{4\pi}{27\sqrt{3}} + \frac{\log(3)}{6} \approx 0.00736862$. So, the intersection of the PPT-set with either of the two sets accounts for less than one-percent of the total probability. (This smallness appears to be very much in line with that exhibited in Figure 3 in [9]—also [3, Figs. 2, 3].)

If we enforce both the MUB and Choi tests for entanglement, but not the PPT constraint, we obtain a probability of $\frac{1}{9} \approx 0.11111$. This doubles to $\frac{2}{9} \approx 0.22222$, if only one of the two tests needs to be met, again without PPT necessarily holding. (“An entanglement witness is an observable detecting entanglement for a subset of states. We present a framework that makes an entanglement witness *twice* [emphasis added] as powerful due to the general existence of a second (lower) bound, in addition to the (upper) bound of the very definition” [10].) Continuing, then, the probability for either of the tests to be met, but not the other, is $\frac{1}{18} \approx 0.05555$.

If, on the other hand, the PPT-constraint is satisfied, but both of the two entanglement tests are failed, the associated probability is $\frac{1}{9}(8 - 3\log(3)) \approx 0.5226847927$.

The intersection is void between those (bound-entangled) states satisfying both PPT and MUB criteria and those (bound-entangled) states satisfying both PPT and Choi criteria. (In their two-qutrit analysis, Gabuldin and Mandilara concluded that the bound-entangled states had “negligible volume and that these form tiny ‘islands’ sporadically distributed over

Constraint Imposed	Probability	Numerical Value
—	1	1.
PPT	$\frac{8\pi}{27\sqrt{3}}$	0.537422
MUB	$\frac{1}{6}$	0.1666667
Choi	$\frac{1}{6}$	0.1666667
PPT \wedge MUB	$-\frac{4}{9} + \frac{4\pi}{27\sqrt{3}} + \frac{\log(3)}{6}$	0.00736862
PPT \wedge Choi	$-\frac{4}{9} + \frac{4\pi}{27\sqrt{3}} + \frac{\log(3)}{6}$	0.00736862
MUB \wedge Choi	$\frac{1}{9}$	0.11111
MUB \vee Choi	$\frac{2}{9}$	0.22222
\neg MUB \wedge Choi	$\frac{1}{18}$	0.05555
MUB \wedge \neg Choi	$\frac{1}{18}$	0.05555
PPT \wedge \neg MUB	$\frac{1}{162} (72 + 8\sqrt{3}\pi - 27 \log(3))$	0.5300534
PPT \wedge \neg Choi	$\frac{1}{162} (72 + 8\sqrt{3}\pi - 27 \log(3))$	0.5300534
PPT \wedge MUB \wedge Choi	0	0
PPT \wedge (MUB \vee Choi)	$-\frac{8}{9} + \frac{8\pi}{27\sqrt{3}} + \frac{\log(3)}{3}$	0.0147372
\neg PPT \wedge MUB	$\frac{1}{3} + \frac{22518\sqrt{3}}{91} + \frac{3888\sqrt{3}}{7\pi} - \frac{10939\pi}{27\sqrt{3}} - \frac{\log(3)}{8}$	0.1592980
\neg PPT \wedge Choi	$\frac{1}{3} + \frac{22518\sqrt{3}}{91} + \frac{3888\sqrt{3}}{7\pi} - \frac{10939\pi}{27\sqrt{3}} - \frac{\log(3)}{8}$	0.1592980
\neg PPT \wedge \neg MUB	$\frac{1}{162} (9(7 + \log(27)) - 8\sqrt{3}\pi)$	0.303279920
\neg PPT \wedge \neg Choi	$\frac{1}{162} (9(7 + \log(27)) - 8\sqrt{3}\pi)$	0.303279920
\neg PPT \wedge \neg MUB \wedge \neg Choi	$\frac{1}{9} (3 \log(3) - 1)$	0.255092985
PPT \wedge \neg MUB \wedge \neg Choi	$\frac{1}{9} (8 - 3 \log(3))$	0.5226847927
PPT \vee (MUB \wedge Choi)	$\frac{1}{81} (9 + 8\sqrt{3}\pi)$	0.648533145

TABLE I: Various Hilbert-Schmidt probabilities for the Hiesmayr-Löffler $d = 3$ two-qutrit model. Notationally, \neg is the negation logic operator (NOT); \wedge is the conjunction logic operator (AND); and \vee is the disjunction logic operator (OR).

the surface of the polytope of separable states” [12]. In a continuous variable study [13], “the tiny regions in parameter space where bound entanglement does exist” were noted”)

In Fig. 3 we show these non-intersecting ragged/craggy/jagged islands of bound-entangled states. (The notion of fractal-type behavior comes to mind.) The bound-entangled prob-

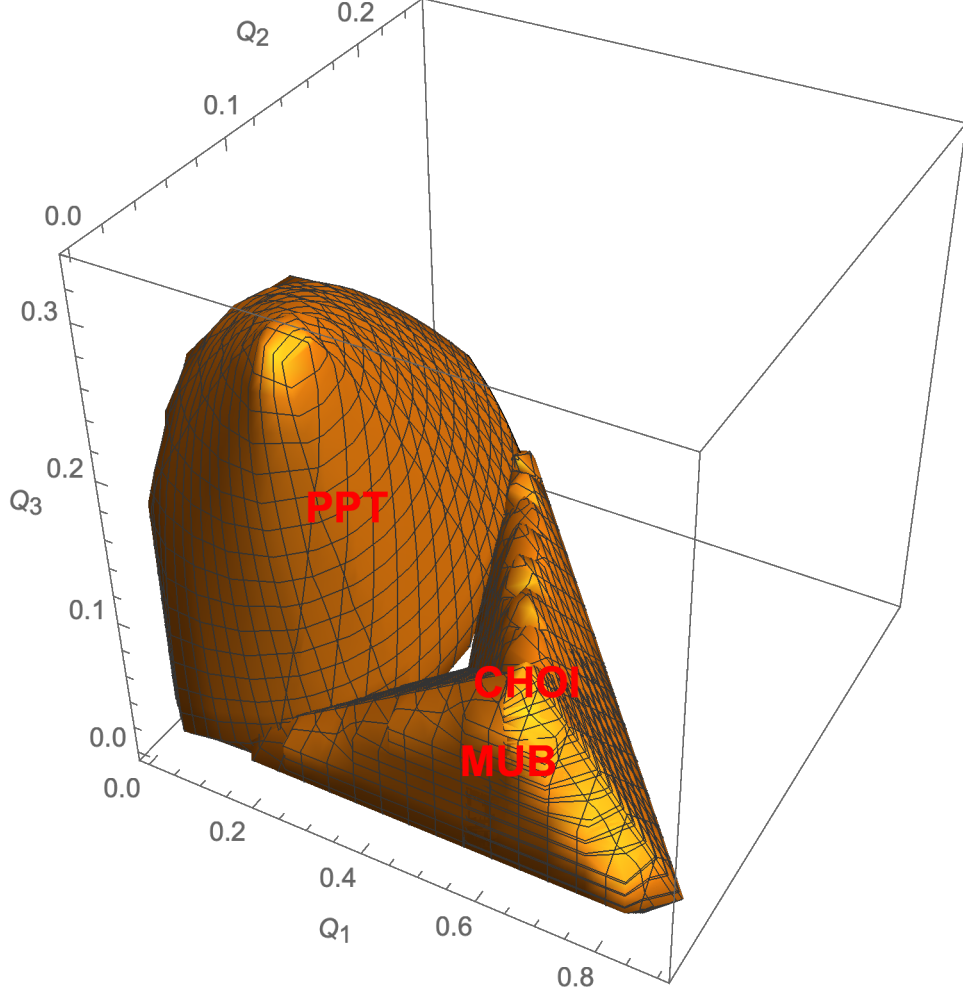


FIG. 2: The largest object is the convex body of PPT states, while the more forward of the other two equal-sized (intersecting) objects is composed of those entangled states revealed by the MUB test, and the more backward-positioned one, composed of those entangled states revealed by the Choi test.

abilities of $-\frac{4}{9} + \frac{4\pi}{27\sqrt{3}} + \frac{\log(3)}{6} \approx 0.00736862$ are equal to 36 times the depicted volumes.

In Fig. 4 we show the effect upon the calculated probability of allowing the right-hand side (zero) of the constraint (11) to instead vary. When the bound is zero—as in (11)—the indicated bound-entangled probability of $-\frac{4}{9} + \frac{4\pi}{27\sqrt{3}} + \frac{\log(3)}{6} \approx 0.00736862$ is obtained. If the bound is further loosened to as high as $\frac{43}{32} \approx 1.34375$, where the associated constraint loses all effect, the curve attains the PPT-probability of $\frac{8\pi}{27\sqrt{3}} \approx 0.537422$. At the other extreme, for a bound as strong as $-\frac{3}{16} \approx -0.1875$, the probability yielded is simply zero. In Fig. 5 we

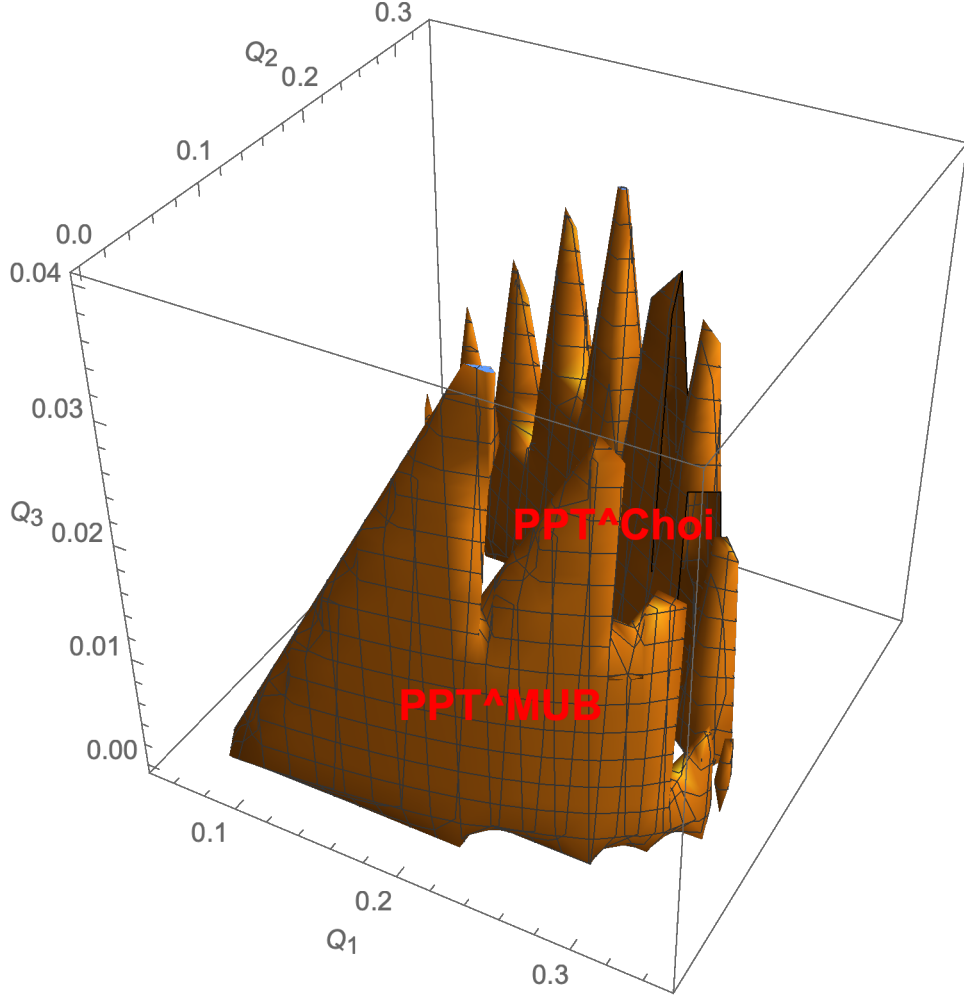


FIG. 3: Jagged islands of bound-entangled states. The $\text{PPT} \wedge \text{MUB}$ island is situated in front of the $\text{PPT} \wedge \text{Choi}$ one. The former is confined to $0 < Q_2 < \frac{1}{9}$ and the latter to $\frac{1}{9} < Q_2 < \frac{1}{3}$.

show the points lying at the boundary between the separable and bound-entanglement states based on the MUB witness, obtained by setting $Q_2 = \frac{1}{3}(Q_1 - 4Q_3)$, so that the inequality constraint (8) becomes an equality.

1. *Extension of Choi witness $W^{(+)}$ to $W^{(+)}(a)$*

From the papers [14, 15] we obtained a general (initially three-parameter $([a, b, c])$ set of entanglement witnesses $W^{(+)}(a)$ (with the Choi witness already employed corresponding to $a = 1$). It was generated by replacing (making use of cyclical permutations of a, b, c) the diagonal entries of the witness (10) by $\{a, b, c, c, a, b, b, c, a\}$. The conditions imposed on the

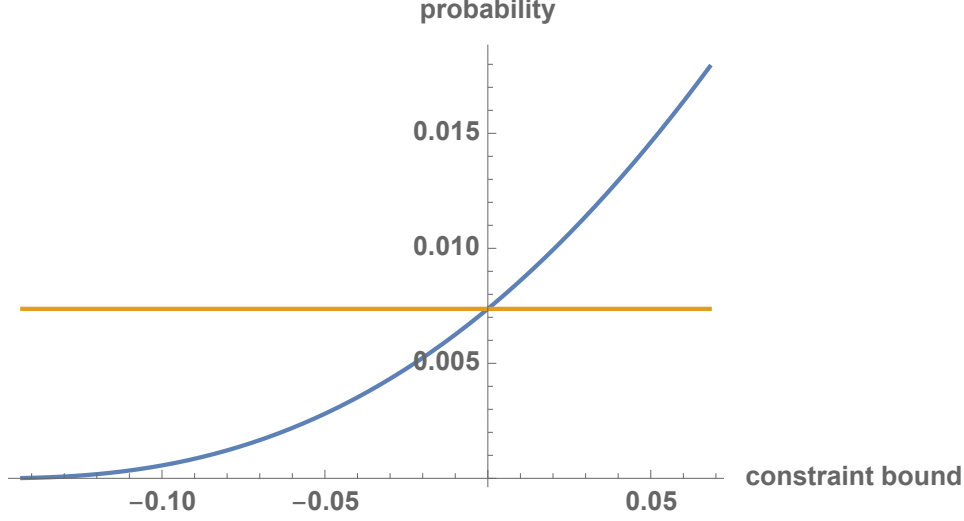


FIG. 4: Probability as a function of the constraint bound $\text{Tr}[W\rho_3]$ imposed on the Choi witness. When the bound is zero—as in (11)—the indicated bound-entangled probability of $-\frac{4}{9} + \frac{4\pi}{27\sqrt{3}} + \frac{\log(3)}{6} \approx 0.00736862$ is obtained.

three parameters are [15, eq. (1)]

$$a + b + c = 2, 0 \leq a \leq 1, b, c \geq 0, bc = (1 - a)^2. \quad (13)$$

To start our associated analyses, for $a = \frac{1}{4}(3 - \sqrt{5})$, we found an entanglement probability of $\frac{5}{132}(5 + \sqrt{5}) \approx 0.274093$ and a bound-entangled probability of 0.00149772192.

Further, we note that $a = \frac{1}{3}$ is the particular case $i = 4$ of [15, eq. (1)]

$$a = \frac{2}{3} \left(\cos\left(\frac{\pi i}{3}\right) + 1 \right), b = \frac{2}{3} \left(-\frac{1}{2}\sqrt{3} \sin\left(\frac{\pi i}{3}\right) - \frac{1}{2} \cos\left(\frac{\pi i}{3}\right) + 1 \right), \quad (14)$$

and

$$c = \frac{2}{3} \left(\frac{1}{2}\sqrt{3} \sin\left(\frac{\pi i}{3}\right) - \frac{1}{2} \cos\left(\frac{\pi i}{3}\right) + 1 \right).$$

For $1 \leq i \leq 5$ the corresponding witness is optimal [15].

Now, for $a = \frac{1}{3}$, we have an entanglement probability of $\frac{125}{486} = \frac{5^3}{2 \cdot 3^5} \approx 0.257202$, with a bound-entangled probability of

$$\frac{-204 + 7 \log(7) + 168\sqrt{3} \cos^{-1}\left(\frac{11}{14}\right)}{1134} \approx 0.00325612294236. \quad (15)$$

The case $a = 1$ yields back our initial Choi witness $W^{(+)}$ analysis, for which a bound-entangled probability of $-\frac{4}{9} + \frac{4\pi}{27\sqrt{3}} + \frac{\log(3)}{6} \approx 0.00736862$ was obtained.

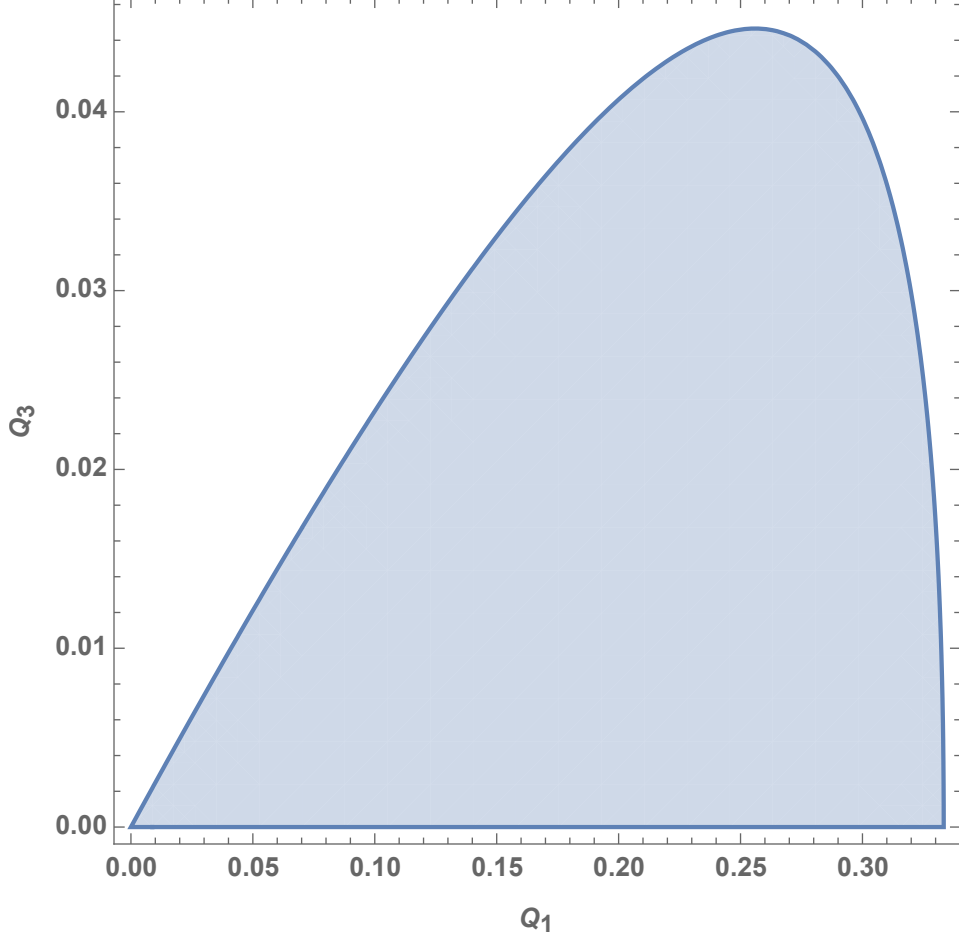


FIG. 5: Points situated at the boundary between the separable and bound-entangled Hiesmayr-Löffler $d = 3$ two-qutrit states, based on the MUB constraint (8), by setting $Q_2 = \frac{1}{3}(Q_1 - 4Q_3)$

More, generally still, the entanglement probabilities for this class of witnesses $W^{(+)}(a)$, are given by (Fig. 6)

$$= \frac{(a-2)^3}{9a^2 - 30a + 27}. \quad (16)$$

a. First one-parameter family of bound-entangled probabilities. Further, the bound-entangled probability obtained by application of the family of generalized Choi witnesses $W^{(+)}(a)$ to the Hiesmayr-Löffler $d = 3$ two-qutrit model is given by the expression (Fig. 7)

$$= \frac{A+B}{54(4-3a)^{3/2}(2a-3)}, \quad (17)$$

where

$$A = 8\sqrt{12-9a} (6a^2 - 17a + 12) \cos^{-1} \left(\frac{a(3a-8)+6}{6-4a} \right)$$

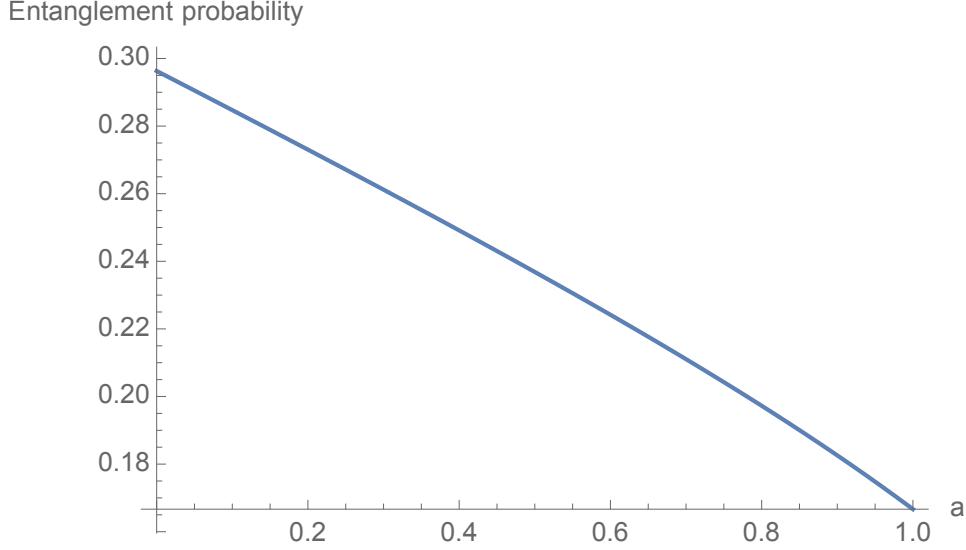


FIG. 6: Probability of entanglement $-\frac{(a-2)^3}{9a^2-30a+27}$ —obtained by application of the family of generalized Choi witnesses $W^{(+)}(a)$ to the Hiesmayr-Löffler $d = 3$ two-qutrit model. The maximum of $\frac{8}{27} \approx 0.296296$ is attained at $a = 0$.

and

$$B = 3\sqrt{a} \left(2(9a^3 - 57a^2 + 108a - 64) + 3(3 - 2a)a \log(9 - 6a) \right).$$

In regard to this formula (17), C. Dunkl remarked: “I have one intuitive observation: the mixture of special functions (including trig) in the answers appears to imply that the boundaries of the sets you are measuring are complicated and have pieces of various properties (e.g. flat, curved ...)”. As an expansion upon this remark (cf. Fig. 3)—suggestive of the jagged-island phenomenon—let us note that the bound-entangled probability function (17) was obtained by the integration of the value 36, firstly of Q_2 over the interval $[\frac{1}{6}(-Q_1 - 2Q_3 + 1) - \frac{1}{6}\sqrt{-3Q_1^2 + 12Q_3Q_1 - 2Q_1 - 4Q_3 + 1}, \frac{1}{6}(-Q_1 - 2Q_3 + 1) - \frac{1}{6}\sqrt{-\frac{((a-2)(3Q_1-1)+6aQ_3)^2}{a(3a-4)}}]$, secondly of Q_3 over the interval $[0, \frac{a(\sqrt{\frac{(3a-4)(3Q_1-1)(3(3a-4)Q_1+4)}{a^2}}+3)+(15-9a)Q_1-5}{9a}]$, and thirdly of Q_1 over $[\frac{-a^2+2a-1}{2a-3}, \frac{1}{3}]$.

In Fig. 8, we display the ratio of the bound-entangled probability (17) to the entanglement probability (16).

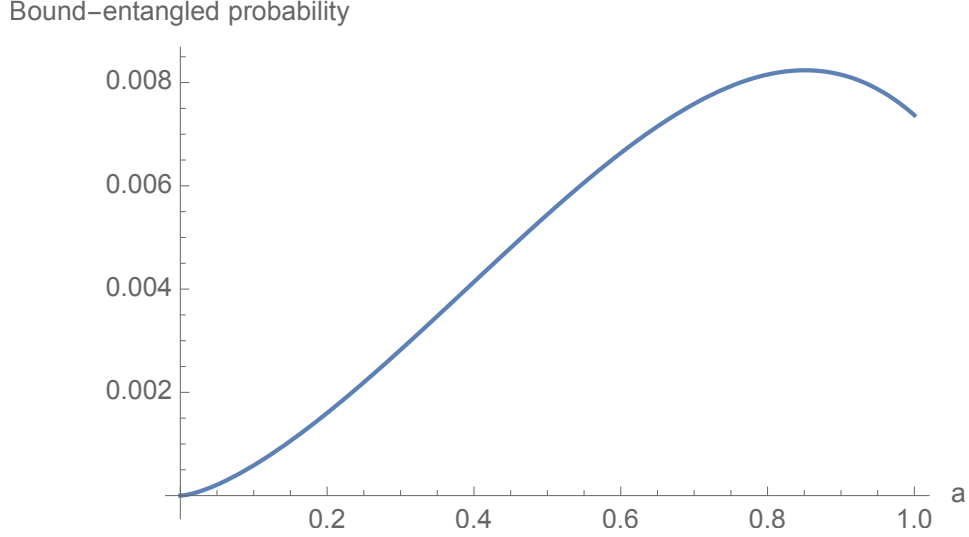


FIG. 7: Probability of bound entanglement (17) obtained by application of the family of generalized Choi witnesses $W^{(+)}(a)$ to the Hiesmayr-Löffler $d = 3$ two-qutrit model. The peak ≈ 0.0082381739 is near $a = 0.8509958326$. (These two values are quite complicated analytically.) At $a = \frac{1}{3}$, the probability is $\frac{-204+7\log(7)+168\sqrt{3}\cos^{-1}(\frac{11}{14})}{1134} \approx 0.00325612294236$. At $a = 1$, the probability is $-\frac{4}{9} + \frac{4\pi}{27\sqrt{3}} + \frac{\log(3)}{6} \approx 0.00736862$ (Table I).

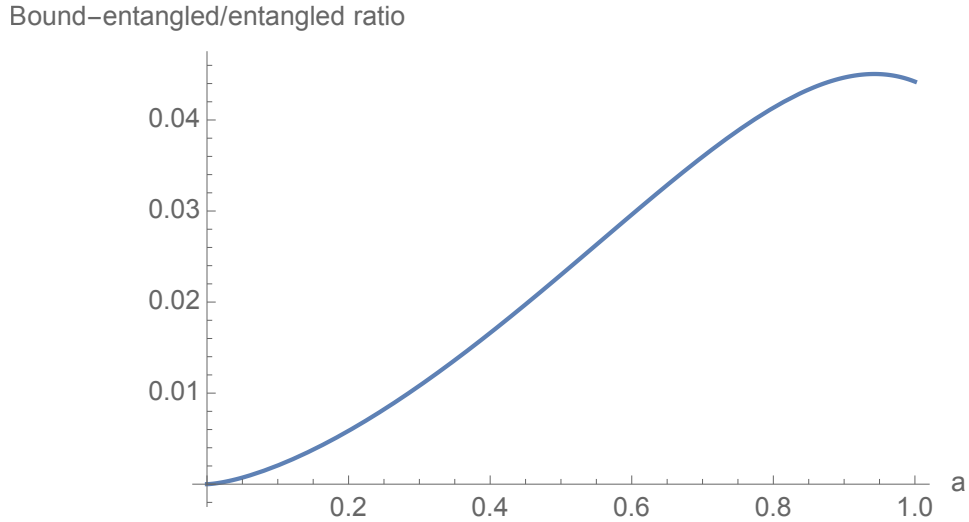


FIG. 8: Ratio of bound-entangled probability to entanglement probability for the Hiesmayr-Löffler $d = 3$ two-qutrit model in terms of the generalized Choi entanglement witness $W^{(+)}(a)$. The peak ≈ 0.0450501588 is near $a = 0.94280530186$.

2. Entanglement witnesses from mutually unbiased bases

Moving on to further forms of witnesses, we observed that for the entanglement witness given in [14, eq. (32)],

$$\frac{1}{3} \left(\begin{array}{ccc|ccc} 4 & \cdot & \cdot & \cdot & -1 & \cdot & \cdot & \cdot & -1 \\ \cdot & 1 & \cdot & \cdot & \cdot & 2 & 2 & \cdot & \cdot \\ \cdot & \cdot & 1 & 2 & \cdot & \cdot & \cdot & 2 & \cdot \\ \hline \cdot & \cdot & 2 & 1 & \cdot & \cdot & \cdot & 2 & \cdot \\ -1 & \cdot & \cdot & \cdot & 4 & \cdot & \cdot & \cdot & -1 \\ \cdot & 2 & \cdot & \cdot & \cdot & 1 & 2 & \cdot & \cdot \\ \hline \cdot & 2 & \cdot & \cdot & \cdot & 2 & 1 & \cdot & \cdot \\ \cdot & \cdot & 2 & 2 & \cdot & \cdot & \cdot & 1 & \cdot \\ -1 & \cdot & \cdot & \cdot & -1 & \cdot & \cdot & \cdot & 4 \end{array} \right), \quad (18)$$

there was no entanglement at all detected for the $d = 3$ Hiesmayr-Löffler model under study here.

This last witness is the particular case $\phi_1 = \phi_2 = \pi, \phi_3 = \phi_4 = 0$ of a family parameterized by an L -dimensional torus ($L = 2, 3, 4$, being the number of MUBs' used in the construction).

As an exercise, we randomly generated values of ϕ_1, ϕ_2, ϕ_3 and $\phi_4 \in [0, 2\pi]$ —and evaluated their (bound and non-bound/free) entanglement probabilities with respect to the $d = 3$ Hiesmayr-Löffler model. Neither of the probabilities generated exceeded the maximum ones indicated ($\frac{8}{27} \approx 0.296296$ and ≈ 0.0082381739 in Figs. 6 and 7).

3. Jafarizadeh-Behzadi-Akbari witnesses

In [8], M. A. Jafarizadeh, N. Behzadi, and Y. Akbari (JBA), constructed “[o]n the basis of linear programming, new sets of entanglement witnesses (EWs) for $3 \otimes 3$ and $4 \otimes 4$ systems”. In the $3 \otimes 3$ case, their two witnesses \mathcal{W}_α and \mathcal{W}'_α were defined over $\alpha \in [\frac{1}{3}, \frac{2}{3}]$ [8, eqs. (17), (18)].

The associated entanglement constraints for the $d = 3$ Hiesmayr-Löffler model took the forms

$$\alpha(-3\alpha Q_1 + (9\alpha - 3)Q_2 + 6\alpha Q_3 + Q_4) < 0, \quad (19)$$

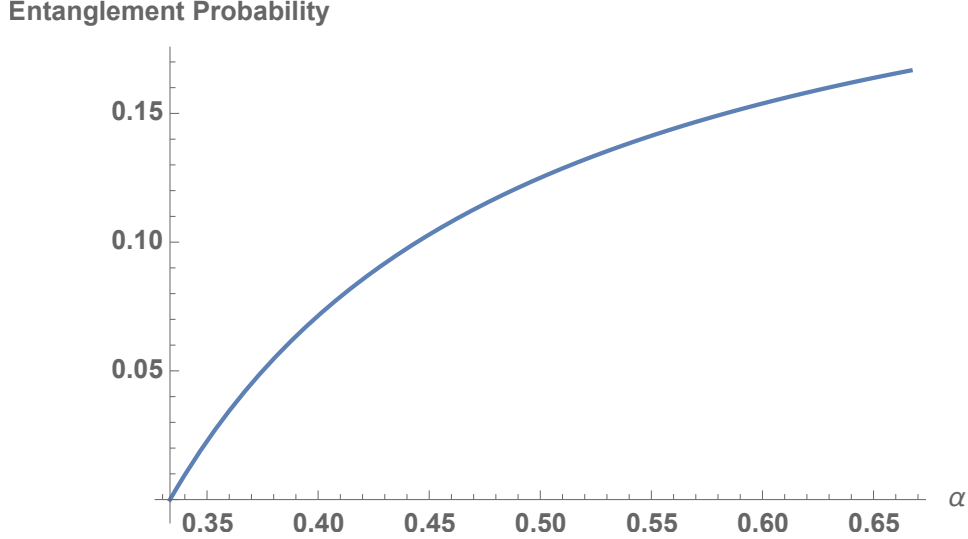


FIG. 9: Identical entanglement probabilities, $\frac{1-3\alpha}{2-12\alpha}$, over $\alpha \in [\frac{1}{3}, \frac{2}{3}]$, for the $d = 3$ Hiesmayr-Löffler model, based on either JBA witness (19) or (20).

and

$$\alpha(3\alpha - 1)(2Q_1 + 3Q_2 - 1) > 2\alpha Q_3, \quad (20)$$

respectively.

The entanglement probabilities for the two witnesses were identical (Fig. 9), being given by

$$\frac{1 - 3\alpha}{2 - 12\alpha}. \quad (21)$$

a. Second one-parameter family of bound-entangled probabilities. The bound-entangled probability (Fig. 10) based on either of these two JBA witnesses is given by the product of

$$\frac{1}{162(6(1 - 3\alpha)\alpha + 1)^2} \quad (22)$$

and

$$8\sqrt{3}\pi(6(1 - 3\alpha)\alpha + 1)^2 - 18(3\alpha - 1)(15\alpha + 2)(6\alpha(3\alpha - 1) - 1) - 6\sqrt{18(1 - 3\alpha)\alpha + 3(3\alpha + 1)^3} \csc^{-1} \left(\frac{3\alpha + 1}{\sqrt{6(1 - 3\alpha)\alpha + 1}} \right).$$

In Fig. 11, we jointly plot a rescaled version of this bound-entangled probability figure based on the JBA witnesses along with that earlier-derived one (Fig. 7) using the generalized Choi witnesses.

Bound-entangled probability

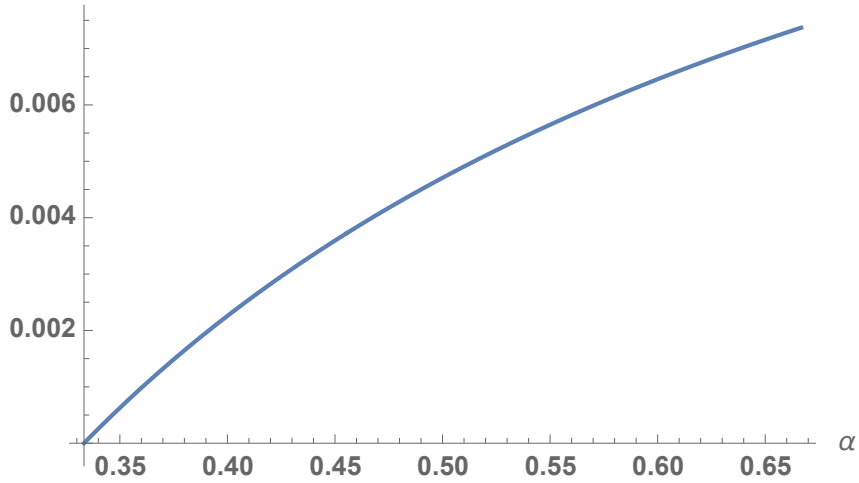


FIG. 10: Bound-entangled probability function (22) for the $d = 3$ Hiesmayr-Löffler model based on either JBA witness \mathcal{W}_α or \mathcal{W}'_α . At $\alpha = \frac{1}{2}$, the probability is $\frac{1}{324} \left(-342 + 16\sqrt{3}\pi + 375\sqrt{6}\text{csch}^{-1} \left(\frac{5}{\sqrt{2}} \right) \right) \approx 0.00470668$, while at $\alpha = \frac{2}{3}$, it is $\frac{1}{162} (8\sqrt{3}\pi + 9(\log(27) - 8)) \approx 0.00736862$.

In Figs. 12 and 13, we show the probabilities of the intersections and unions of the bound-entangled regions revealed through use of the one-parameter families of generalized JBA and Choi witnesses.

In Fig. 14 we show a pair of jagged islands for $\alpha = \frac{3}{5}$.

It was commented upon in [8] that the expectation value of \mathcal{W}_α “with respect to the all separable states is positive hence it can be an EW for $\alpha \in [\frac{1}{3}, \frac{2}{3}]$ ”. The formula (22) was derived assuming these restrictions—but we have observed that if we take the limit $\alpha \rightarrow \infty$, it attains the value

$$\frac{1}{324} \left(-90 + 16\sqrt{3}\pi + 3\sqrt{6} \sinh^{-1} \left(\sqrt{2} \right) \right) \approx 0.0169299. \quad (23)$$

Possibly this is not an achievable (or near-achievable) bound-entanglement probability measurement. For $\alpha = \frac{2}{3}$, the formula (22) has the considerably lesser value $\frac{1}{162} (8\sqrt{3}\pi + 9(\log(27) - 8)) \approx 0.00736862$.

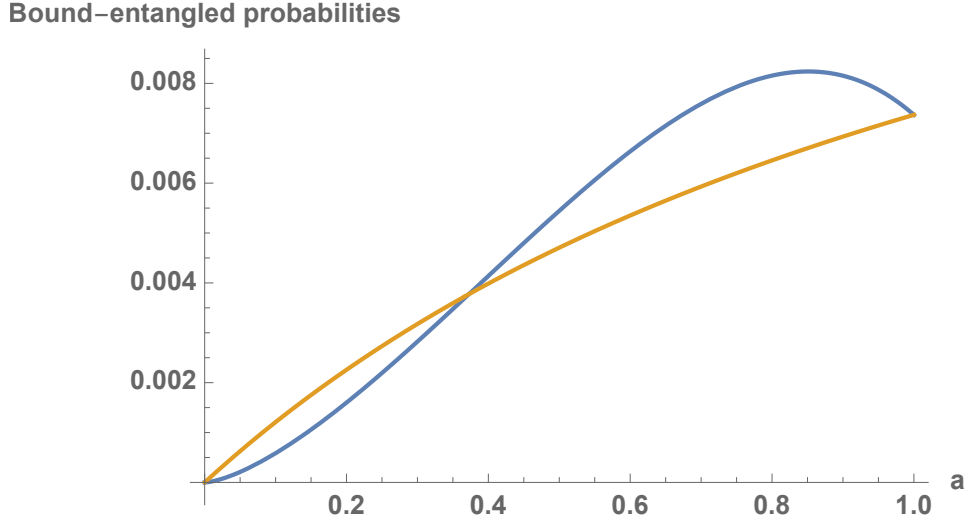


FIG. 11: Rescaled ($\alpha \rightarrow \frac{a+1}{3}$) JBA-based Fig. 10 plotted along with generalized-Choi-based Fig. 7. The curves intersect at $a \approx 0.372519577$ with a common bound-entangled probability ≈ 0.00377346692 .

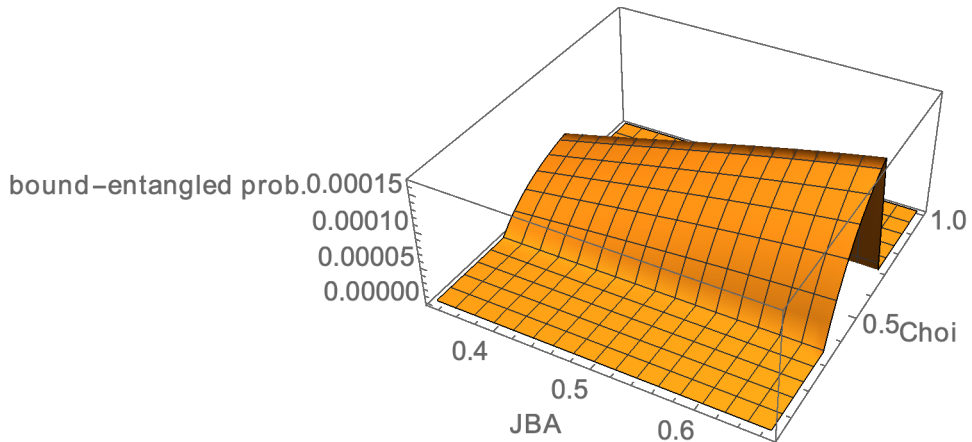


FIG. 12: Probabilities of the *intersections* of the bound-entangled regions revealed through use of the one-parameter ($\alpha \in [\frac{1}{3}, \frac{2}{3}], a \in [0, 1]$) families of generalized JBA and Choi witnesses ($d = 3$)

C. Two-ququart analyses ($d = 4$)

Similarly to our $d = 3$ analyses (sec. II A), in the $d = 4$ (two-ququart) framework, to transform between the sixteen nonnegative parameters ($c[k, l] \geq 0$, with $k, l = 0, \dots, 3$), summing to 1, for the full/original magic simplex [4, sec. 4] and the four (q_1, q_2, q_3, q_4) of the

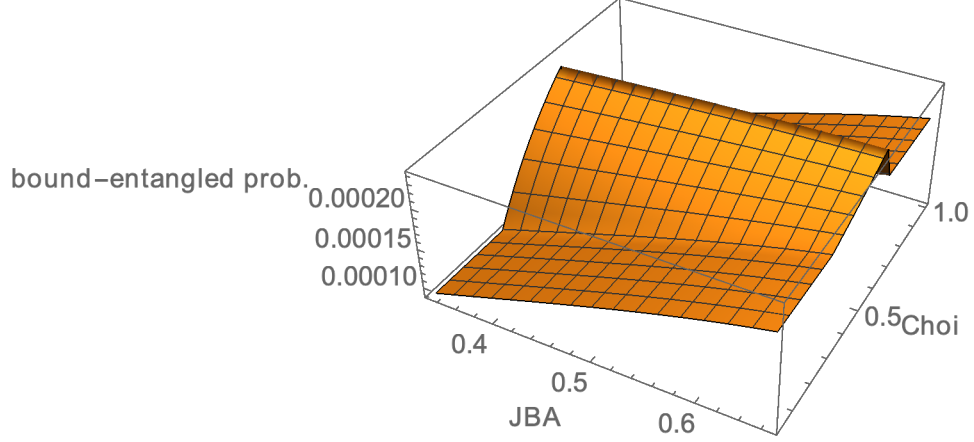


FIG. 13: Probabilities of the *unions* of the bound-entangled regions revealed through use of the one-parameter ($\alpha \in [\frac{1}{3}, \frac{2}{3}]$, $a \in [0, 1]$) families of generalized JBA and Choi witnesses ($d = 3$)

Hiesmayr-Löffler subset, we must take

$$c[0, 0] = \frac{1}{880} (75q_1 - 11q_2 - 55q_3 - 55q_4 + 55) \equiv Q_1, \quad (24)$$

and

$$c[k, l] = \frac{1}{880} (-5q_1 - 11q_2 + 165q_3 - 55q_4 + 55) \equiv Q_2 \quad (25)$$

for $\{k, l\} = \{0, 1\}, \{1, 1\}, \{2, 1\}, \{3, 1\}$, and

$$c[k, l] = \frac{1}{880} (-5q_1 - 11q_2 - 55q_3 + 165q_4 + 55) \equiv Q_3, \quad (26)$$

for $\{k, l\} = \{0, 2\}, \{1, 2\}, \{2, 2\}, \{3, 2\}$, and

$$c[k, l] = \frac{-15q_1 + 143q_2 - 165q_3 - 165q_4 + 165}{2640} \equiv Q_4 \quad (27)$$

for $\{k, l\} = \{1, 0\}, \{2, 0\}, \{3, 0\}$.

If we employ Q_1, Q_2, Q_3, Q_4 as our four principal variables, rather than q_1, q_2, q_3, q_4 in the Hiesmayr-Löffler parameterization (1), using the linear transformations,

$$q_1 = \frac{11}{4} (5Q_1 + 4Q_2 + 4Q_3 + 3Q_4 - 1), \quad q_2 = \frac{15}{4} (Q_1 + 4Q_2 + 4Q_3 + 7Q_4 - 1), \quad (28)$$

and

$$q_3 = Q_1 + 8Q_2 + 4Q_3 + 3Q_4 - 1, \quad q_4 = Q_1 + 4Q_2 + 8Q_3 + 3Q_4 - 1,$$

our ensuing analyses simplify greatly. The requirement that ρ_4 is a nonnegative definite density matrix—or, equivalently, that its sixteen leading nested minors are nonnegative—takes

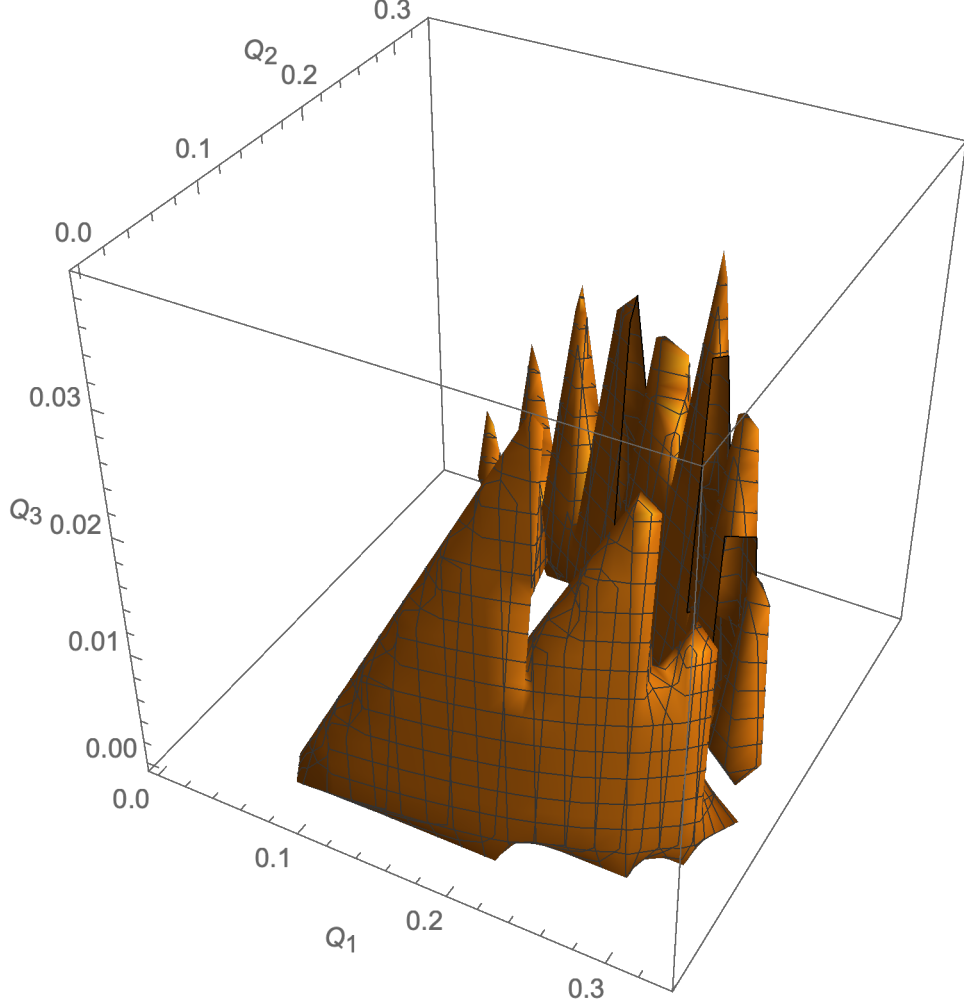


FIG. 14: The anterior "jagged island" represents the bound entanglement based on the Jafarizadeh-Behzadi-Akbari witness \mathcal{W}_α and the posterior one that based on \mathcal{W}'_α for the $d = 3$ (two-qutrit) Hiesmayr-Löffler magic simplex. The parameter α has been set to $\frac{3}{5}$.

the form

$$Q_1 > 0 \wedge Q_4 > 0 \wedge Q_2 > 0 \wedge Q_3 > 0 \wedge Q_1 + 4(Q_2 + Q_3) + 3Q_4 < 1. \quad (29)$$

The constraint that the partial transpose of ρ_4 is nonnegative definite is

$$Q_3 > 0 \wedge Q_1 + 3Q_4 > 0 \wedge Q_1 + 4(Q_2 + Q_3) + 3Q_4 < 1 \wedge Q_1^2 + 4Q_2Q_1 + Q_4^2 \quad (30)$$

$$+ 16Q_2(Q_2 + Q_3) + 12Q_2Q_4 < 4Q_2 + 2Q_1Q_4 \wedge (Q_1 - Q_4)^2 < 16Q_3^2.$$

With these formulas, we are able to establish that the corresponding PPT-probability is $\frac{1}{2} + \frac{\log(2-\sqrt{3})}{8\sqrt{3}} \approx 0.404957$ (again, quite elegant, but seemingly of a different analytic form than the $d = 3$ counterpart of $\frac{8\pi}{27\sqrt{3}}$).

it to a clearly challenging one-dimensional integration. However, we were apparently able to obviate this formidable task by doing a numerical integration using a `WorkingPrecision`→ 24 option. Inputting the result obtained to the WolframAlpha website, an exact value of

$$\frac{8 \log(2)}{27} - \frac{59}{288} \approx 0.00051583, \quad (33)$$

was suggested, which matched the numerical output to considerably more than twenty decimal places. (As a matter of, at least, initial curiosity, the WolframAlpha site also suggested— to equally high-precision—an exact value of $\frac{1}{864}(-64b_4(2) - 177)$, where “ $b_4(2)$ is the Madelung constant $b_4(2)$ ”. Equating the two exact suggested values implies that $b_4(2) = -4 \log(2)$. We could not immediately confirm this identity, but the [mathworld.wolfram.com Madelung Constants](http://mathworld.wolfram.com/MadelungConstants) page informs us that, seemingly relatedly, $b_2(2) = -\pi \log(2)$.) At a later point, though, N. Tessore was able to fully confirm the validity of (33) through strictly symbolic integration .

D. Chruściński also indicated that a modification of W_{2quart} s could be achieved by replacing the sixteen diagonal entries of (31) with the sequence $\{2, 1, 0, 0, 0, 2, 1, 0, 0, 0, 2, 1, 1, 0, 0, 2\}$. The associated entanglement constraint is, then,

$$4Q_2 + 9Q_4 < Q_1. \quad (34)$$

Doing so, leads to a reduced (from $\frac{2}{9}$) entanglement (without PPT required) probability of $\frac{1}{8}$, but a substantially increased bound-entangled probability of [17]

$$\frac{24 \operatorname{csch}^{-1}\left(\frac{8}{\sqrt{17}}\right)}{17\sqrt{17}} - \frac{91}{544} \approx 0.002187. \quad (35)$$

This is 4.24019 times greater than the bound-entangled probability, $\frac{8 \log(2)}{27} - \frac{59}{288}$, obtained with the initially used two-ququart witness (31). (For several efforts to graphically represent the results of the immediately preceding set of two-ququart analyses, along the lines of Fig. 2, see [11]—in particular, the animation there—obtained by variation of the Q ’s—of MichaelE2.)

The joint imposition of the two last constraints (32) and (34) gives a (lesser) bound-entanglement probability of

$$-\frac{571}{2448} + \frac{5 \log(2)}{54} + \frac{24 \operatorname{csch}^{-1}\left(\frac{8}{\sqrt{17}}\right)}{17\sqrt{17}} \approx 0.000395295. \quad (36)$$

It would be of interest to embed this last pair of two-ququart entanglement witnesses provided by Chruściński into a parameterized family, similarly to the case of the two-qutrit

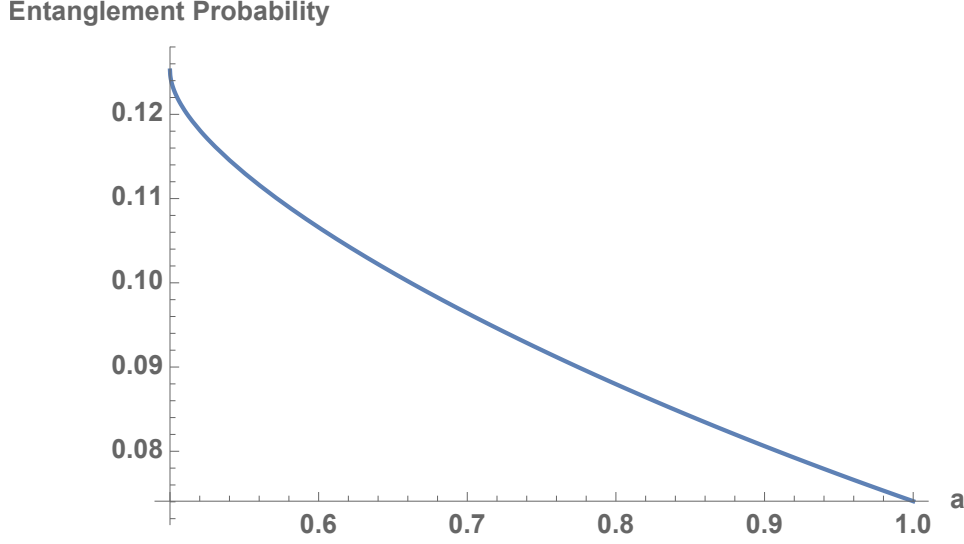


FIG. 15: Entanglement probability $\frac{(a-3)^4}{2(a-7)(2a-5)(-2a+\sqrt{-4(a-2)a-3+7})}$ for class I of $W[a, b, c, d]$. At $a = \frac{1}{2}$, the probability is $\frac{625}{4992} \approx 0.1252$, and at $a = 1$, it is $\frac{2}{27} \approx 0.0740741$.

and in class II (Fig. 16),

$$\frac{(a-3)^4 \left(a + \sqrt{(1-a)a-4} \right)}{8(a-7)(a-2)(a(2a-9)+16)}. \quad (41)$$

These two functions are both equal to $\frac{625}{4992} \approx 0.1252$ at $a = \frac{1}{2}$. The intersection of the two entanglement tests at that point, then, yields a probability of $\frac{512}{4125} \approx 0.124121212$, while their union gives $\frac{512}{3135} \approx 0.163317384$.

At $a = 1$, the intersection of the two tests yields a probability of $\frac{2}{16335} \approx 0.000122436$, while their union gives $\frac{32}{165} \approx 0.193939$. At that same point, the case I entanglement probability is $\frac{2}{27} \approx 0.0740741$, and the case II entanglement probability is $\frac{1}{9} \approx 0.11111$.

In Figs. 17 and 18, we show the entanglement probabilities arising from the intersection and union of classes I and II, while in Fig. 19, we show the ratio of the union curve to the intersection curve. (We were able to obtain a formula for the former curve—but quite large in nature.)

To conclude this section, let us note that for the witness W_4 specified by [21, eq. (8.4)], we obtained an entanglement (without PPT-requirement) probability of $\frac{8}{25} \approx 0.32$ for the $d = 4$ Hiesmayr-Löffler states, but no (with PPT-requirement) bound-entanglement. Further, for the witness W_4^{spin} specified by [21, eq. (8.26)], no entanglement at all was detected.

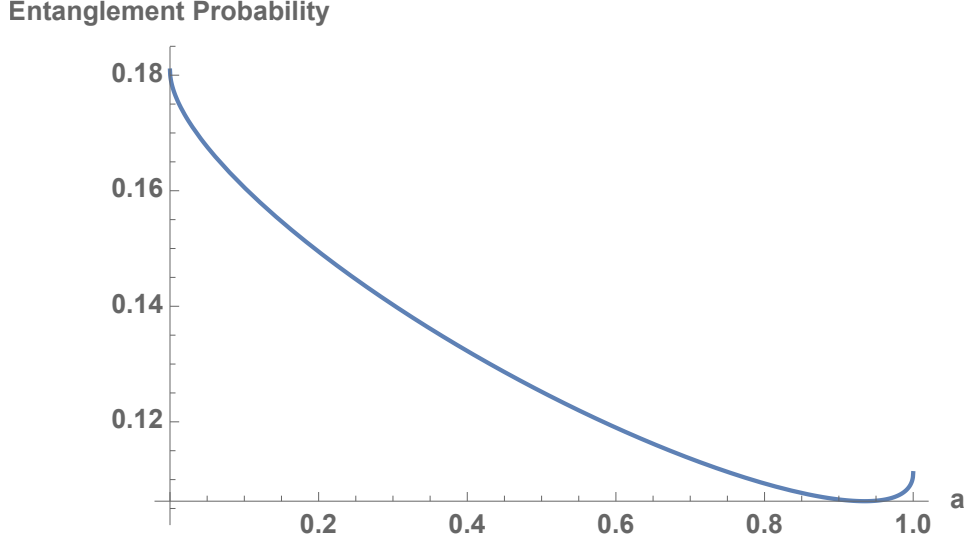


FIG. 16: Entanglement probability $\frac{(a-3)^4(a+\sqrt{(1-a)a-4})}{8(a-7)(a-2)(a(2a-9)+16)}$ for class II of $W[a, b, c, d]$. At $a = 0$, the probability is $\frac{81}{448} \approx 0.180804$, and at $a = 1$, it is $\frac{1}{9} \approx 0.11111$. The curve reaches a minimum of ≈ 0.1062629 at $a \approx 0.9347153$.

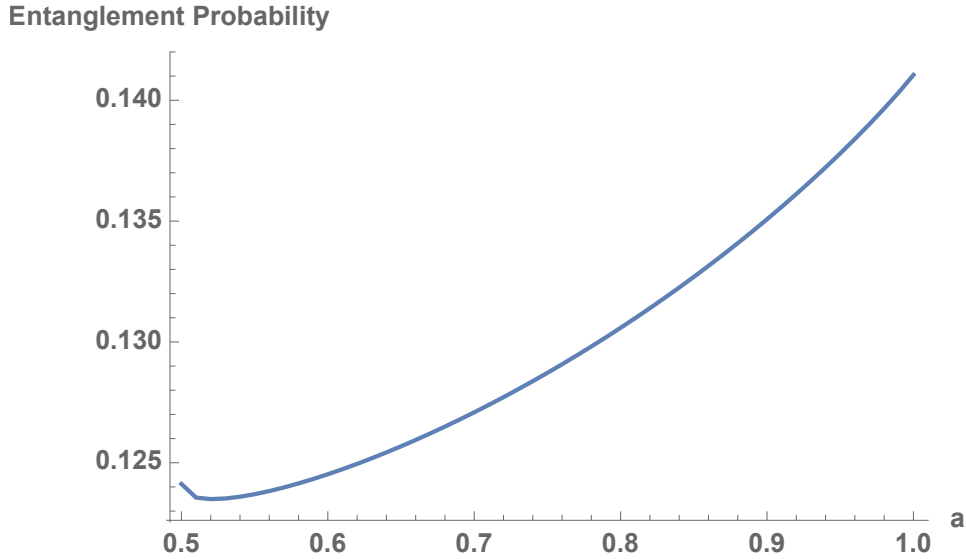


FIG. 17: Entanglement probability for intersection of classes I and II for entanglement witness $W[a, b, c, d]$ (37)

2. JBA witnesses

Analogously to our analyses in sec. II B 3, we constructed for the $d = 4$ Hiesmayr-Löffler model, the entanglement constraints for the pair of Jafarizadeh-Behzadi-Akbari witnesses

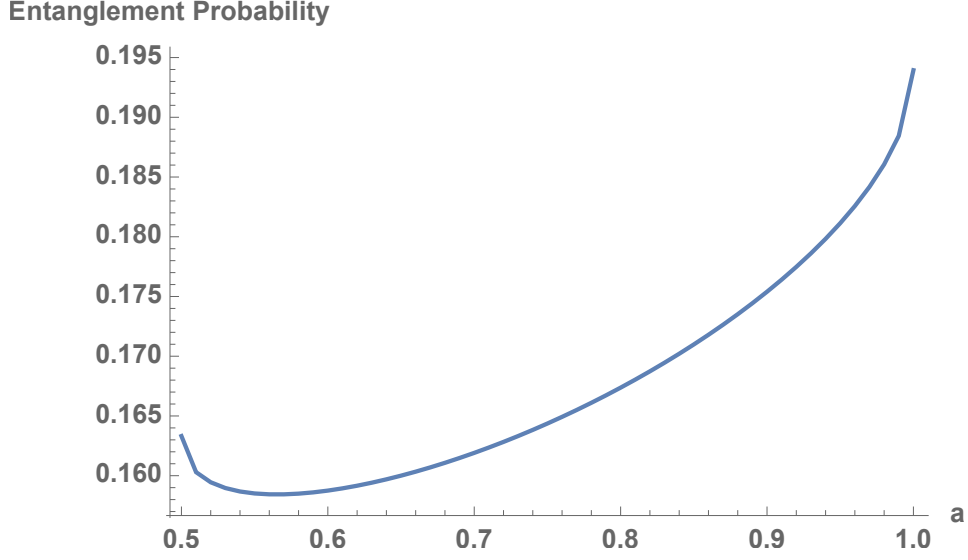


FIG. 18: Entanglement probability for union of classes I and II for entanglement witness $W[a, b, c, d]$ (37)

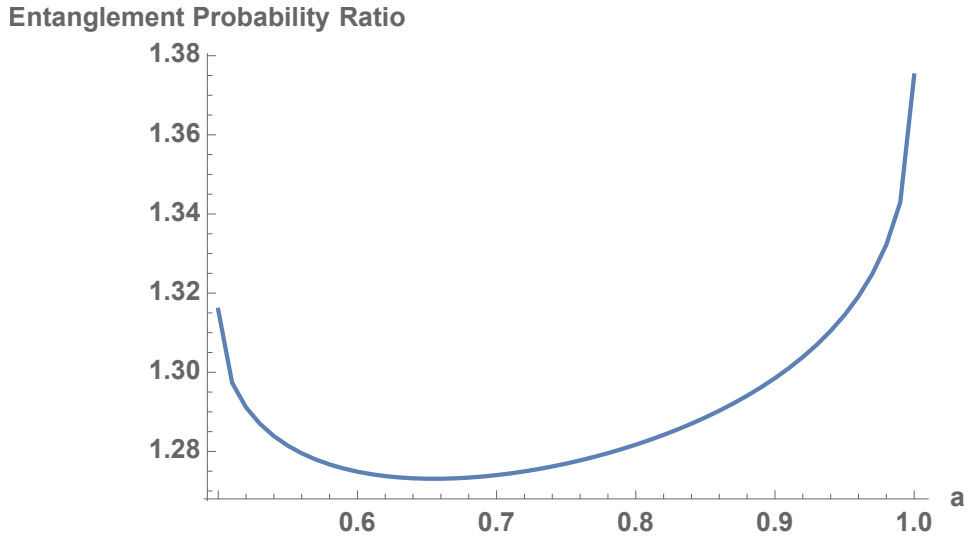


FIG. 19: Ratio of union to intersection of classes I and II for entanglement witness $W[a, b, c, d]$ (37)

\mathcal{W}_α and \mathcal{W}'_α given in [8, eqs.(38) and (39)]. These took the forms,

$$3Q_4 < \frac{(4\alpha - 1)(Q_1 - 4Q_2)}{4\alpha}, \quad (42)$$

and

$$3\alpha Q_4 < \alpha(4\alpha - 1)(2Q_1 + 4Q_2 + 4Q_3 - 1), \quad (43)$$

respectively.

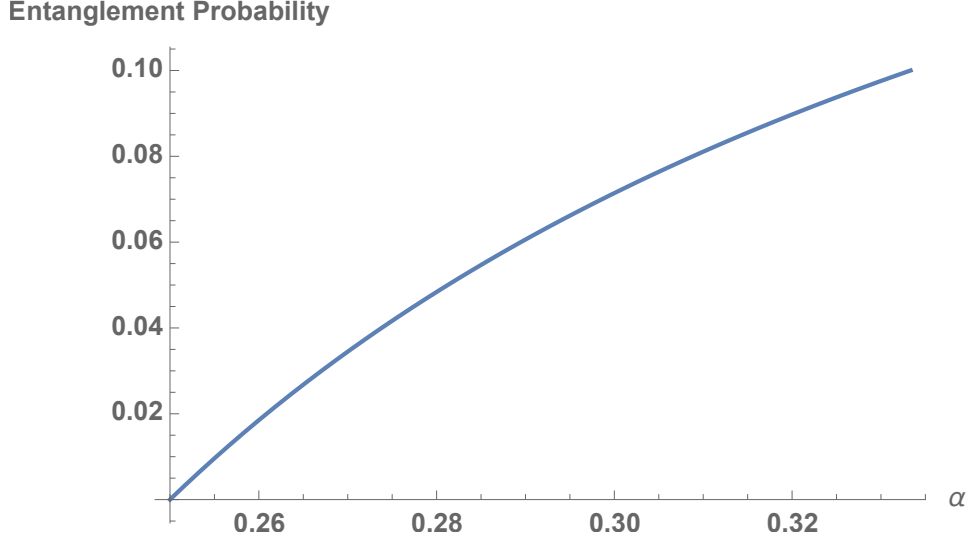


FIG. 20: Two-ququart entanglement probability for the $d = 4$ Hiesmayr-Löffler model, $\alpha \in [\frac{1}{4}, \frac{1}{3}]$, given by (44)

The entanglement probability based on either \mathcal{W}_α or \mathcal{W}'_α took the form

$$\frac{1 - 4\alpha}{2 - 16\alpha} \quad (44)$$

In Fig. 20, we show this probability curve. The (intersection) probability that both entanglement constraints are satisfied is $\frac{1-4\alpha}{3(8\alpha-1)}$, while the (union) probability that at least one of the two is satisfied is $\frac{2-8\alpha}{3-24\alpha}$.

a. Third one-parameter family of bound-entangled probabilities. Now, in Fig. 21, we show the bound-entangled probability based on either the two-ququart JBA witnesses \mathcal{W}_α or \mathcal{W}'_α . This is given by

$$\frac{A + B + C}{32(4\alpha - 1)^{5/2}(20\alpha + 1)^{7/2}}, \quad (45)$$

where

$$A = (-2\alpha - 1)(32\alpha + 1)(16(1 - 5\alpha)\alpha + 1)^2 \sqrt{\frac{6}{4\alpha - 1} + 5},$$

$$B = 27\alpha(8\alpha + 1)^3(16\alpha(10\alpha + 1) + 1) \cosh^{-1}\left(\frac{12\alpha}{8\alpha + 1}\right)$$

and

$$C = -3(8\alpha + 1)^4(2\alpha(80\alpha + 23) + 1) \operatorname{sech}^{-1}\left(\sqrt{\frac{16\alpha + 2}{20\alpha + 1}}\right).$$

At $\alpha = \frac{3}{8} \approx 0.375$ (outside $[\frac{1}{4}, \frac{1}{3}]$), the value is identical to the bound-entangled probability

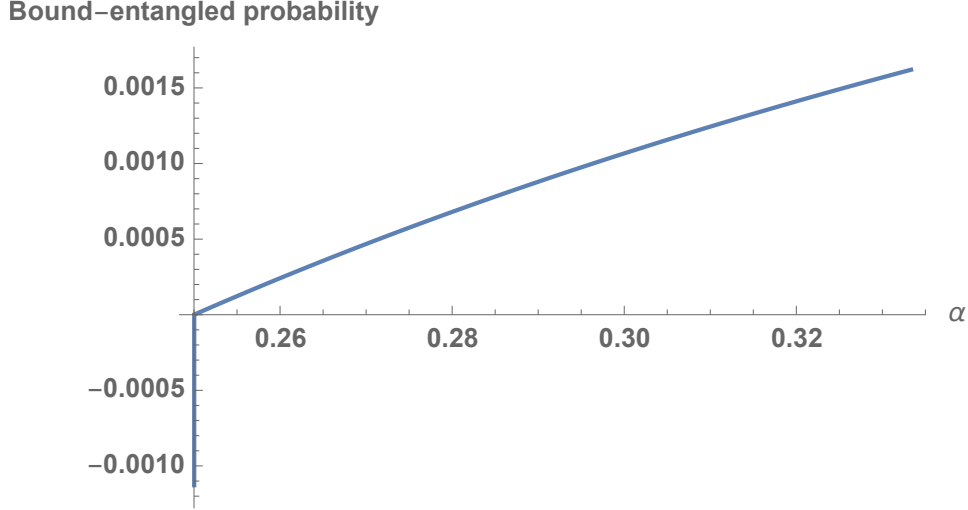


FIG. 21: Two-ququart bound-entangled probability function (45) for the $d = 4$ Hiesmayr-Löffler model, using either the JBA witness \mathcal{W}_α or \mathcal{W}'_α , over $\alpha \in [\frac{1}{4}, \frac{1}{3}]$.

$\frac{24\text{csch}^{-1}\left(\frac{8}{\sqrt{17}}\right)}{17\sqrt{17}} - \frac{91}{544} \approx 0.00218722$, reported above in eq. (35), with respect to the indicated modification of the entanglement witness $W_{2ququarts}$ (31). For given $\alpha \in [\frac{1}{4}, \frac{1}{3}]$, the two witnesses \mathcal{W}_α and \mathcal{W}'_α appear to form disjoint bound entanglement islands (cf. Fig. 3).

In Fig. 22 we show such a pair of islands for $\alpha = \frac{7}{24}$ and $Q_4 = \frac{1}{384}$, while in Fig. 23 we show such a pair of islands for $\alpha = \frac{1}{3}$ and $Q_1 = \frac{1}{6}$.

The formula (45) was derived assuming $\alpha \in [\frac{1}{4}, \frac{1}{3}]$ —as seemed suggested in [8] (the authors claiming that the witnesses are non-decomposable [nd] there). Nevertheless, it appears to hold—as for $\alpha = \frac{3}{8}$ —as well for $\alpha > \frac{1}{3}$. In the limit $\alpha \rightarrow \infty$, it attains the value

$$- \frac{5\sqrt{5} + \log(8) - 27 \log(3 + \sqrt{5}) + 24(\log(2) + \text{csch}^{-1}(2))}{200\sqrt{5}} \approx 0.00728067. \quad (46)$$

We are not aware of whether or not this is an achievable (or near-achievable) bound-entanglement probability measurement. But, for $\alpha = \frac{1}{3}$, the formula (45) has the considerably

lesser value $\frac{-92575 + \frac{7798329 \cosh^{-1}\left(\frac{12}{11}\right)}{\sqrt{23}} - \frac{13484361 \cosh^{-1}\left(\sqrt{\frac{23}{22}}\right)}{\sqrt{23}}}{389344} \approx 0.00162026$.

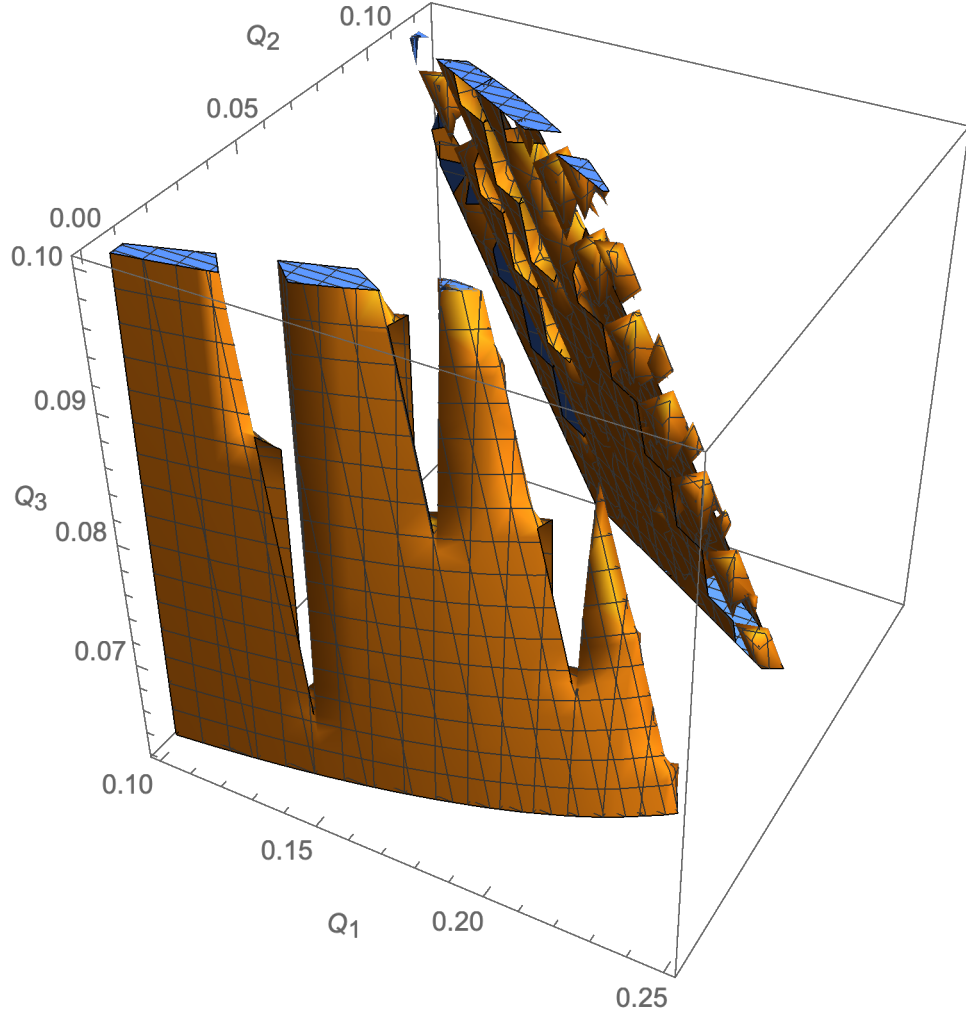


FIG. 22: The anterior "jagged island" represents the bound entanglement for the $d = 4$ (two-quart) Hiesmayr-Löffler magic simplex revealed by the Jafarizadeh-Behzadi-Akbari witness \mathcal{W}_α and the posterior one, that shown by \mathcal{W}'_α . The parameter α has been set to $\frac{7}{24}$ and Q_4 to $\frac{1}{384}$.

III. REALIGNMENT ANALYSES OF HIESMAYR-LÖFFLER MAGIC SIMPLICES

A. Two-qutrit ($d = 3$) case

Application of the realignment (CCNR) test for entanglement [22, 23] yielded an entanglement probability of $\frac{1}{81} (27 + \sqrt{3} \log(97 + 56\sqrt{3})) \approx 0.445977$ and an exact bound-entangled probability of $\frac{2}{81} (4\sqrt{3}\pi - 21) \approx 0.0189035$, considerably larger than the 0.00736862 and 0.00325613 reported above. The realignment constraint that, if satisfied, ensures entanglement

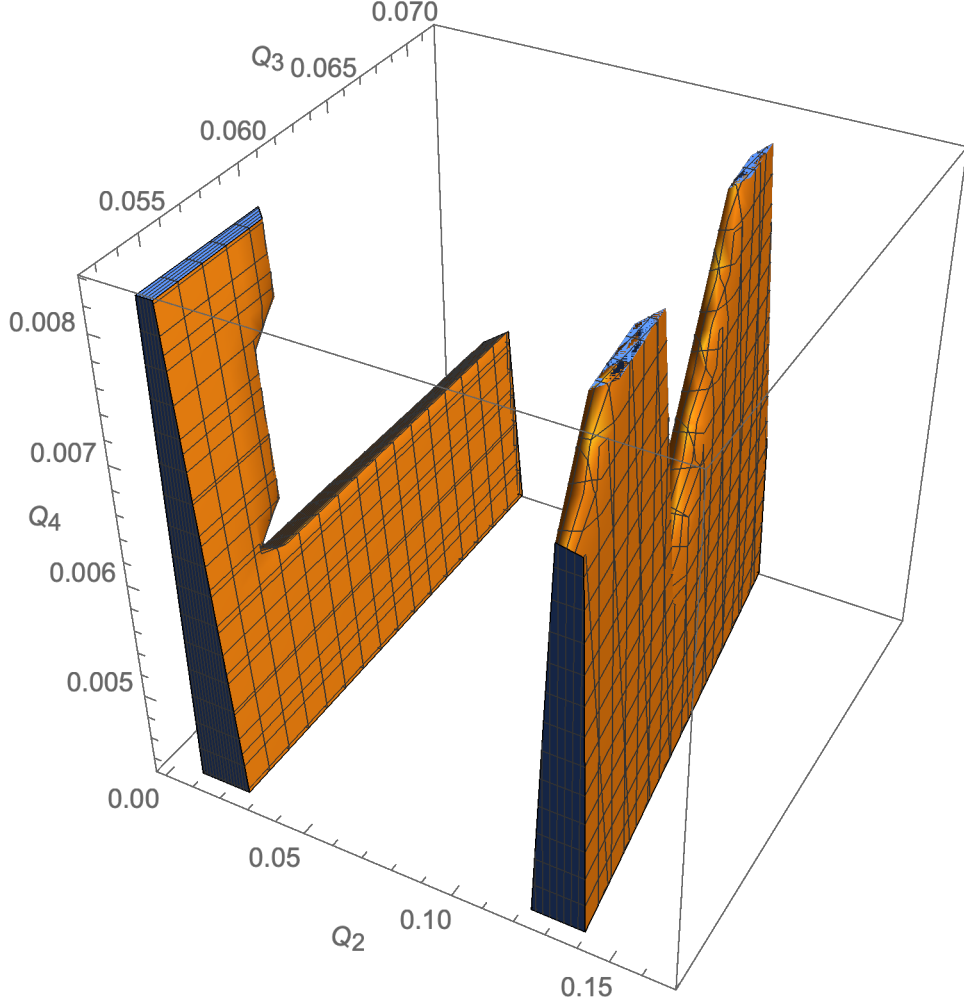


FIG. 23: The left-positioned island represents the bound entanglement based on the Jafarizadeh-Behzadi-Akbari witness \mathcal{W}_α and the right-side one that based on \mathcal{W}'_α for the $d = 4$ (two-quart) Hiesmayr-Löffler magic simplex. The parameter α has been set to $\frac{1}{3}$ and Q_1 to $\frac{1}{6}$ —so as to yield a three-dimensional image.

is

$$\frac{2}{3}\sqrt{-9Q_2 - 6Q_3 + 3(Q_1^2 + (3Q_2 + 4Q_3 - 1)Q_1 + 9Q_2^2 + 4Q_3^2 + 6Q_2Q_3) + 1} \quad (47)$$

$$1/3 + |Q_1 - Q_3| > 1.$$

The bound-entanglement islands obtained by enforcing this constraint are displayed in Fig. 24. (It is interesting to note that the region of *free* entanglement also, in fact, separates into two—not as severely jagged—islands of its own.) These realignment islands completely contain the corresponding Choi and MUB islands, with an additional probability of $\frac{1}{27}(10 - 9\log(3)) \approx$

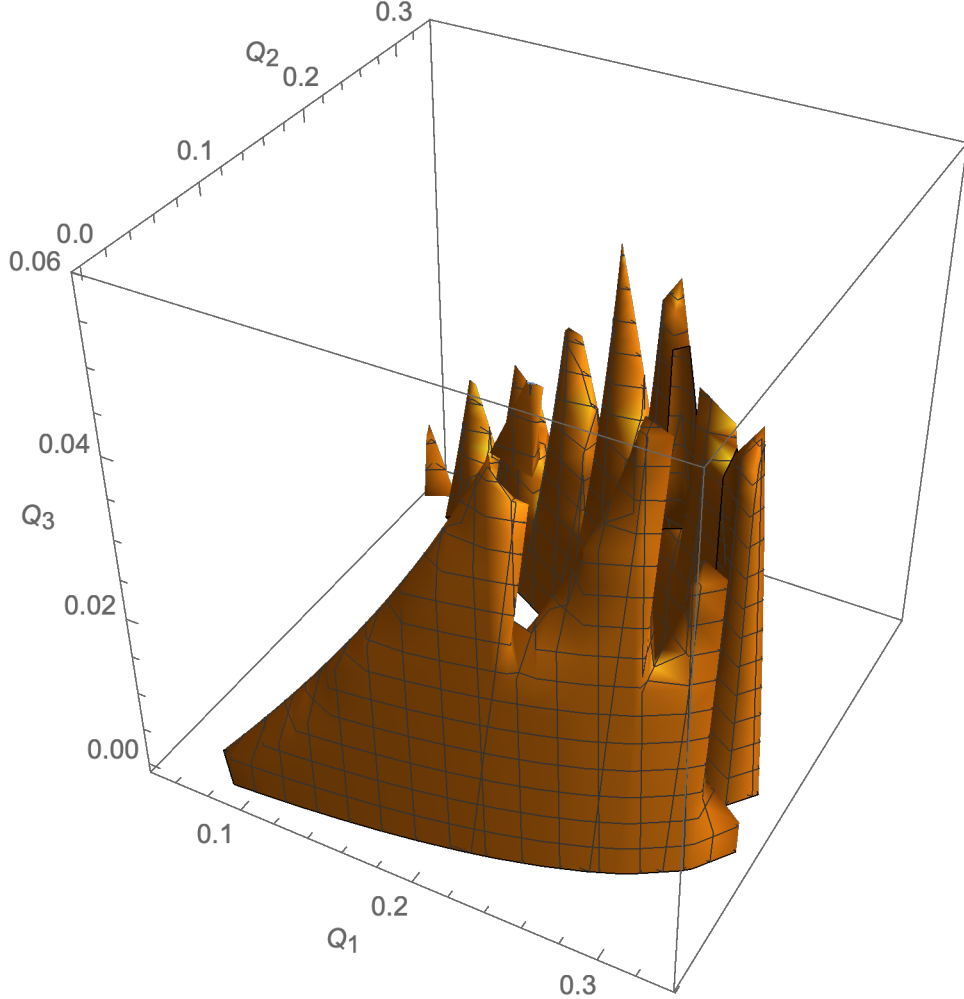


FIG. 24: Islands of bound entanglement for $d = 3$ Hiesmayr-Löffler magic simplex model obtained on the basis of the realignment criterion for entanglement

0.00416627. This (highly fragmented) domain of additional bound-entangled probability found through use of the realignment criterion, but by neither the Choi nor the MUB witnesses is shown in Fig. 25.

We also implemented the entanglement detection criterion (ESIC) based on symmetric informationally complete positive operator-valued measures (SIC POVMs) [23]. We found it to be equivalent to the realignment (CCNR) test.

Motivated by the recent preprint, “Bound entangled states fit for robust experimental verification” [6], we found that the CCNR reached a maximum of $\frac{7}{6}$ at $Q_1 = \frac{1}{4}, Q_2 = \frac{1}{24}(3 - \sqrt{5}), Q_3 = 0$. (In the original Hiesmayr-Löffler coordinates, this converts to $q_1 = \frac{5}{24}(\sqrt{5} - 3), q_2 = -1 - \frac{\sqrt{5}}{3}, q_3 = -\frac{\sqrt{5}}{4}$.) It would be interesting to further analyze this result

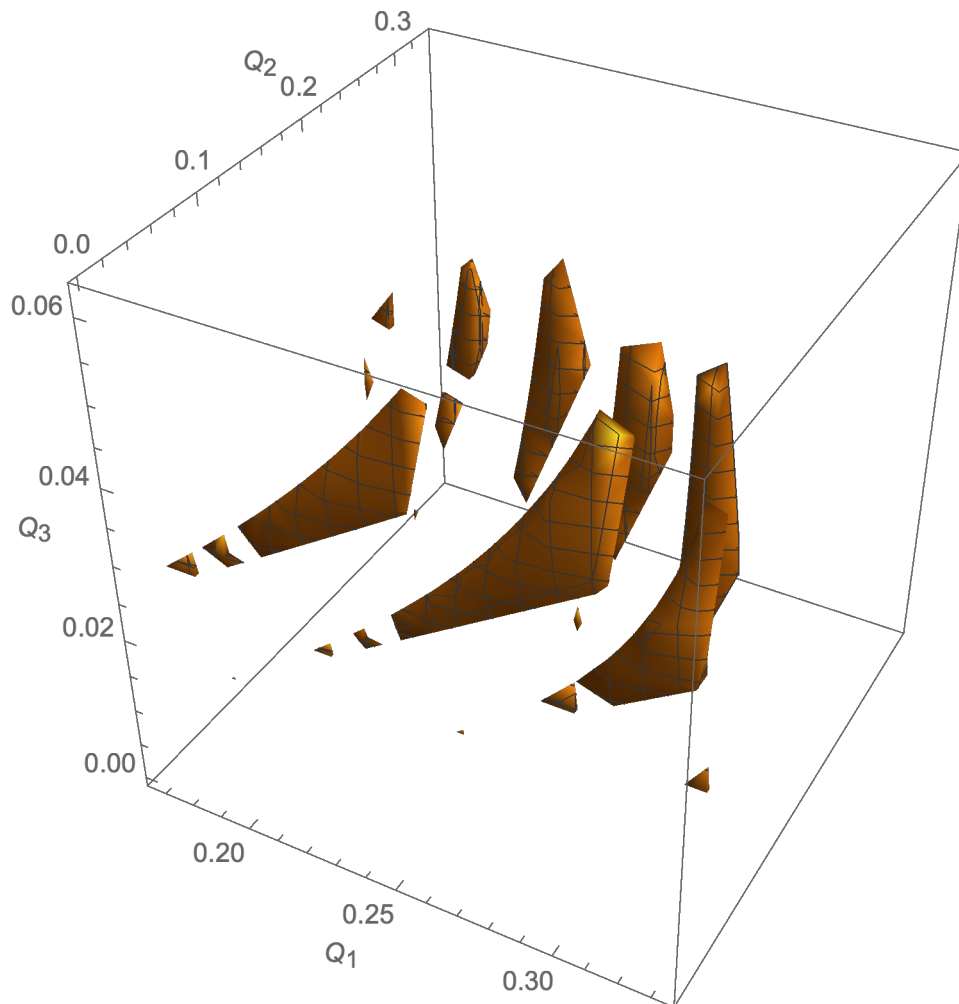


FIG. 25: That part-of probability $\frac{1}{27}(10 - 9\log(3)) \approx 0.00416627$ —of the total realignment criterion bound entanglement (Fig. 24), not found by either the Choi or MUB witnesses.

in the framework of [6], to ascertain how robust—in terms of their criteria—this state is for experimental verification. The (rank-7) density matrix in question takes the form (zeros

being represented by dots)

$$\left(\begin{array}{ccc|ccc|ccc} \frac{1}{12} & \cdot & \cdot & \cdot & \frac{1}{12} & \cdot & \cdot & \cdot & \frac{1}{12} \\ \cdot & \frac{1}{24} (3 - \sqrt{5}) & \cdot \\ \cdot & \cdot & \frac{1}{24} (3 + \sqrt{5}) & \cdot & \cdot & \cdot & \cdot & \cdot & \cdot \\ \cdot & \cdot & \cdot & \frac{1}{24} (3 + \sqrt{5}) & \cdot & \cdot & \cdot & \cdot & \cdot \\ \frac{1}{12} & \cdot & \cdot & \cdot & \frac{1}{12} & \cdot & \cdot & \cdot & \frac{1}{12} \\ \cdot & \cdot & \cdot & \cdot & \cdot & \frac{1}{24} (3 - \sqrt{5}) & \cdot & \cdot & \cdot \\ \cdot & \cdot & \cdot & \cdot & \cdot & \cdot & \frac{1}{24} (3 - \sqrt{5}) & \cdot & \cdot \\ \cdot & \frac{1}{24} (3 + \sqrt{5}) & \cdot \\ \frac{1}{12} & \cdot & \cdot & \cdot & \cdot & \frac{1}{12} & \cdot & \cdot & \frac{1}{12} \end{array} \right). \quad (48)$$

However, undermining the initially presumed robustness of this state is the observation that three of the eigenvalues of its partial transpose are zero, so any perturbation of the state might lead to negative eigenvalues of the partial transpose, and thus its departure from the PPT domain.

B. Two-ququart ($d = 4$) case

Here, we observed free entanglement and bound-entangled probability CCNR-based estimates of 0.4509440211445637 and 0.01265489845176, respectively.

IV. GENERALIZED HORODECKI STATE ANALYSES

At the conclusion of their paper [8], Jafarizadeh, Behzadi, and Akbari consider generalized Horodecki states of the form $\rho_i = \sum_{i=1}^n a_i O_i$, where the O_i 's are unit-trace orthogonal operators. These were used as a basis for constructing EWs, in particular, the pair of witnesses \mathcal{W}_α and \mathcal{W}'_α we have employed above in certain two-qutrit (sec. II B 3) and two-ququart (sec. II C 2) analyses. (Let us also note that Chruściński and Rutkowski have provided a multi-parameter family of 2-qudit PPT entangled states which generalize the celebrated Horodecki-state [7].)

A. Two-qutrit case

Following the suggested approach of JBA for obtaining generalized Horodecki states, in the two-qutrit instance, we have found a PPT-probability of $\frac{1}{27} (4\sqrt{3}\pi - 9) \approx 0.4278$. The entanglement probability with either of the two witnesses is $\frac{1}{2}$. The bound-entangled probability for either witness is $\frac{1}{27} (2\sqrt{3}\pi - 9) \approx 0.0697322$ for $\alpha \in [\frac{1}{3}, \frac{2}{3}]$.

B. Two-ququart case

In the two-ququart generalized Horodecki case, the PPT-probability is $\frac{1}{3} \approx 0.3333$. The entanglement probability with either witness is $\frac{1}{2}$ —again, independently of α . The bound-entangled probability with either witness is $\frac{1}{24} \approx 0.0416667$ for $\alpha \in [\frac{1}{4}, \frac{1}{3}]$.

In Fig. 26 we show a pair of jagged bound-entanglement islands. Six times the displayed volume for each island gives the bound-entanglement probability of $\frac{1}{24}$. (These plots are independent of α .)

C. Two-ququint case

For the 5×5 two-ququint (25×25 density matrices) scenario, the entanglement probability is simply again $\frac{1}{2}$, independently of α , for the two witnesses. (This case is not explicitly discussed in [8], and we have followed their discussions of the previous lower-dimensional instances.) The PPT-probability is approximately 0.33734924124312192527. The bound-entangled probability is ≈ 0.0370662 for $\alpha > \frac{1}{5}$.

It would be of interest to investigate the relations between the JBA generalized Horodecki states we have analyzed and those put forth by Chruściński and Rutkowski [7].

V. FULL-DIMENSIONAL MAGIC SIMPLICES NUMERICAL ANALYSES

A. Two-qutrits

Moving on from the $d = 3$ Hiesmayr-Löffler model, we examined the original 8-dimensional “magical” simplex of Bell states of bipartite qutrits studied by Baumgartner, Hiesmayr and Narnhofer [3, 4].

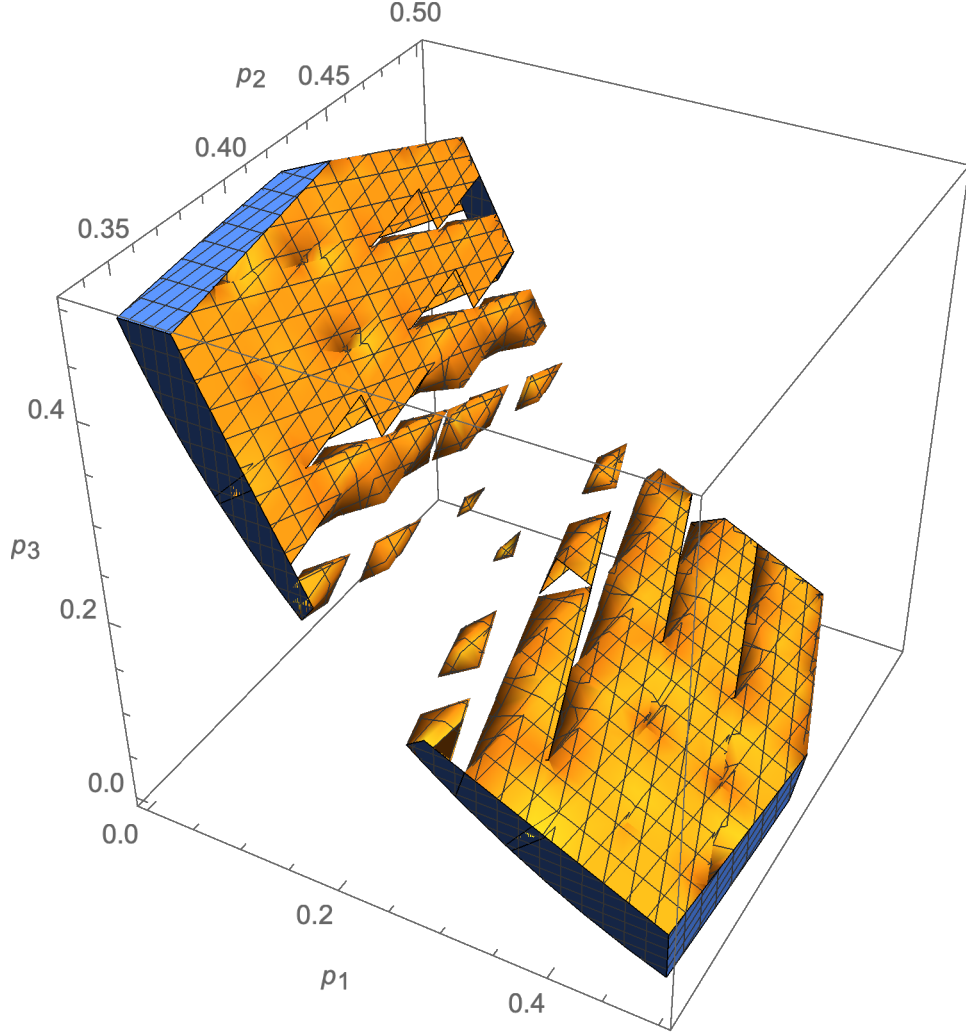


FIG. 26: The upper “jagged island/archipelago” represents the bound entanglement based on the Jafarizadeh-Behzadi-Akbari witness \mathcal{W}_α and the lower one that based on \mathcal{W}'_α for the two-ququart generalized Horodecki states.

In Fig. 27, we plot—using the interesting (golden-ratio-related) “quasi-random” procedure (we have been recently employing [24]) of Martin Roberts [25, 26]—two sets of estimates of the associated Hilbert-Schmidt PPT-probability. One (symmetrically) fixes the Roberts parameter α_0 at $\frac{1}{2}$ (which may lead to superior estimates), and the other at zero. Large numbers of realizations—5,820,000,000 realizations in the former case, and 6,260,000,000 in the latter—were used. The two estimates obtained were 0.39338785 and 0.39339143, respectively. A well-fitting conjecture for the underlying exact value—of a seemingly similar nature to the $d = 3$ Hiesmayr-Löffler counterpart of $\frac{8\pi}{27\sqrt{3}}$ —is $\frac{7\pi}{25\sqrt{5}} \approx 0.3933896249$. (In particular, the

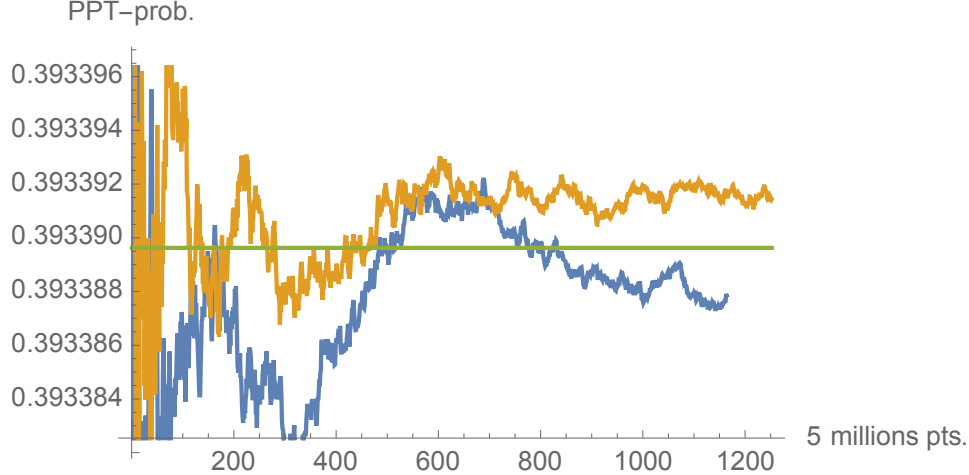


FIG. 27: A pair of (quasi-random) PPT-probability estimates for the 8-dimensional magical simplex of Bell states of bipartite qutrits. The last recorded estimates are 0.39338785 (Roberts parameter $\alpha_0 = \frac{1}{2}$) and 0.39339143 ($\alpha_0 = 0$). The plotted value $\frac{7\pi}{25\sqrt{5}} \approx 0.3933896249$ provides a close fit, with the weighted average of the two estimates being 0.3933897072. We note that the Hiesmayr-Löffler $d = 3$ counterpart is $\frac{8\pi}{27\sqrt{3}} \approx 0.537422$.

average of the two estimates appears to very strongly converge in this direction—with the last recorded average agreeing with the conjecture to six decimal places.)

In a supplementary analysis to these two, now using a Roberts parameter of $\alpha_0 = \frac{1}{3}$, together with 280,000,000 million realizations, we obtained an estimate of 0.393381, plus, additionally, an estimate of 0.00011335 for the associated bound-entangled probability based on the Hiesmayr-Löffler mutually-unbiased-bases criterion (9) of

$$I_4 = 3c[0, 0] + c[0, 1] + 2c[0, 2] + c[1, 1] + 2c[1, 2] + c[2, 1] + 2c[2, 2] > 2. \quad (49)$$

Let us here recall that for the Hiesmayr-Löffler $d = 3$ counterpart, the bound-entangled probability was found to be considerably greater, that is, $-\frac{4}{9} + \frac{4\pi}{27\sqrt{3}} + \frac{\log(3)}{6} \approx 0.00736862$, than 0.000113354.

B. Two-ququarts

For the 15-dimensional magic simplex of Bell states of bipartite ququarts, two Hilbert-Schmidt PPT-probability quasi-random-based estimates, employing approximately one hun-

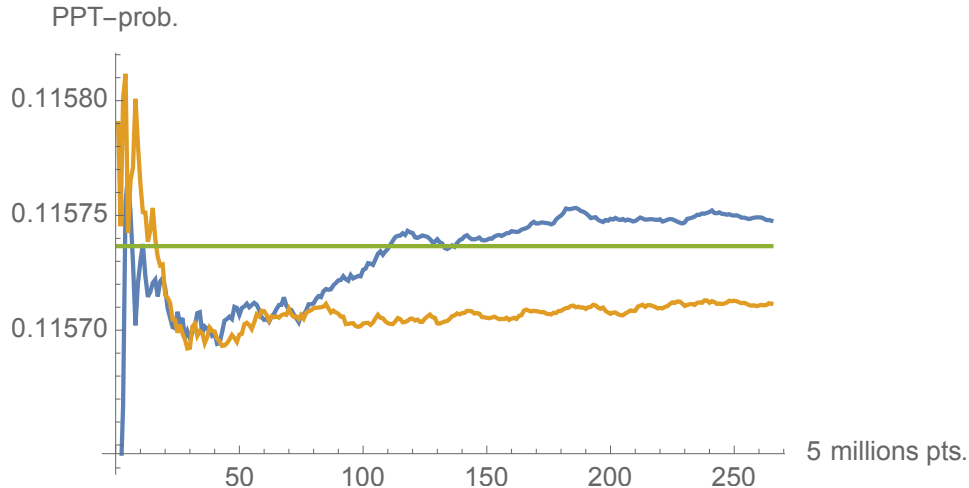


FIG. 28: A pair of (quasi-random) PPT-probability estimates for the 15-dimensional magical simplex of Bell states of bipartite ququarts. The last recorded estimates are 0.1157477026 (Roberts parameter $\alpha_0 = \frac{1}{4}$) and 0.1157115381 ($\alpha_0 = \frac{3}{4}$). Also shown is a conjectured value of $\frac{1}{8} + \frac{\log(3-\sqrt{5})}{13\sqrt{5}} \approx 0.115737$. We note that the Hiesmayr-Löffler $d = 4$ counterpart is $\frac{1}{2} + \frac{\log(2-\sqrt{3})}{8\sqrt{3}} \approx 0.404957$.

dred seventy million realizations each, were 0.115717 ($\alpha_0 = \frac{1}{2}$) and 0.115778 ($\alpha_0 = 0$). The Hiesmayr-Löffler counterpart is $\frac{1}{2} + \frac{\log(2-\sqrt{3})}{8\sqrt{3}} \approx 0.404957$.

At this point—due to certain technical issues—we undertook a parallel set of analyses (however, shifting the Roberts parameters from 0 and $\frac{1}{2}$ to $\frac{1}{4}$ and $\frac{3}{4}$). Additionally, now we recorded whether or not the realignment test [22] for entanglement was passed. In Fig. 28, we plot the two sets of estimates of the associated Hilbert-Schmidt PPT-probability. An interesting candidate value is $\frac{1}{8} + \frac{\log(3-\sqrt{5})}{13\sqrt{5}} \approx 0.115737$.

Further, in Fig. 29, we plot the two sets of estimates of the associated Hilbert-Schmidt entanglement probability based on the realignment criterion.

Also, in Fig. 30, we display the pairs of estimates of the Hilbert-Schmidt bound-entangled probability based on the realignment criterion. A conjecture of $\frac{1}{750} \approx 0.00133333$ can be advanced, in this regard.

VI. FURTHER DISCUSSION

It has been established that for the two-rebit, rebit-retrit and two-retrit X -states (the density matrices for which, by definition, have their only nonzero entries along their diagonal

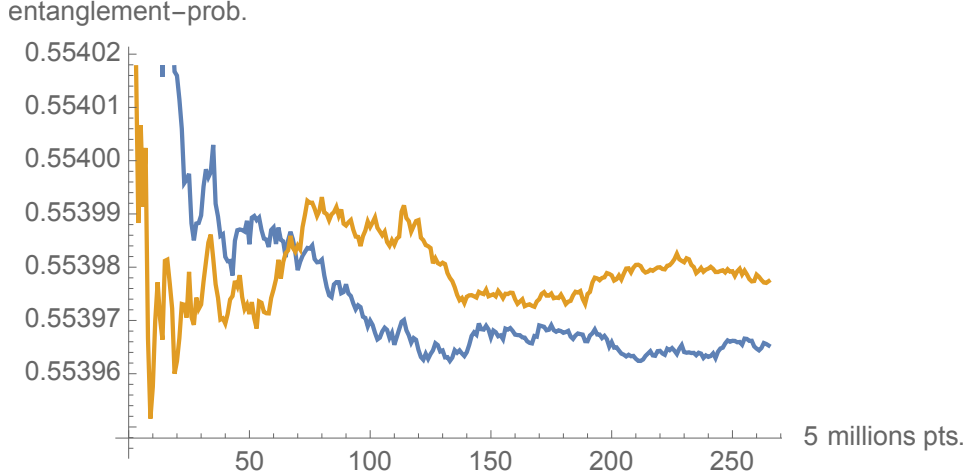


FIG. 29: A pair of (quasi-random) entanglement-probability estimates—based on the realignment criterion—for the 15-dimensional magical simplex of Bell states of bipartite ququarts. The last recorded estimates are 0.5539652981 (Roberts parameter $\alpha_0 = \frac{1}{4}$) and 0.5539773751 ($\alpha_0 = \frac{3}{4}$).

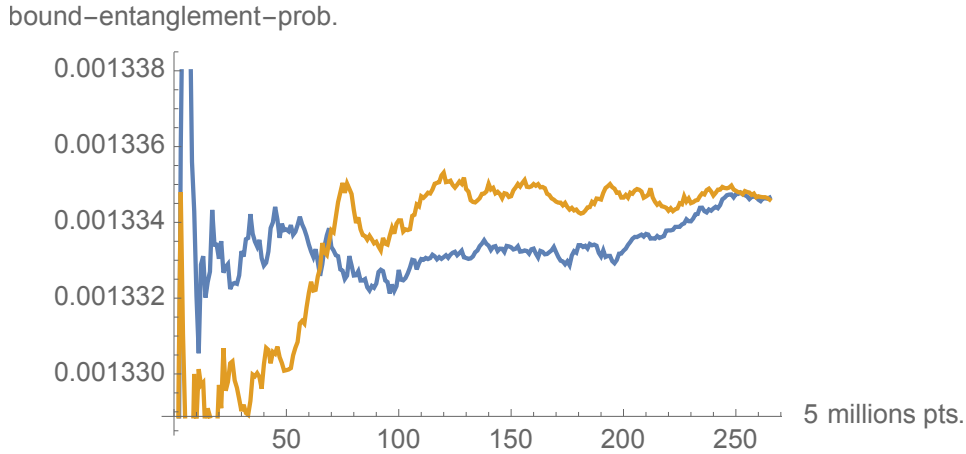


FIG. 30: A pair of (quasi-random) bound-entanglement-probability estimates—based on the realignment criterion—for the 15-dimensional magical simplex of Bell states of bipartite ququarts. The last recorded estimates are 0.001334655094 (Roberts parameter $\alpha_0 = \frac{1}{4}$) and 0.001334600000 ($\alpha_0 = \frac{3}{4}$). A conjecture of $\frac{1}{750} \approx 0.00133333$ can be advanced.

and anti-diagonal [27]), the Hilbert-Schmidt separability/PPT probabilities are all equal to $\frac{16}{3\pi^2} \approx 0.54038$ for the two-rebit, rebit-retrit and two-retrit X -states (cf. [28]). Numerical and exact analyses of ours strongly indicated that among the (9×9) two-retrit PPT-states, none is bound entangled in terms of the Hiesmayr-Löffler MUB $I_d > 2$ criterion. But the question

of whether there are bound-entangled X -states should be addressed more thoroughly than so far has been done.

There certainly are many more directions in which efforts to determine probabilities of bound-entangled states can be directed (cf. [29, sec.IV.C] for a 2×4 density matrix analysis, and [30] for multipartite issues).

Much research has been devoted to the determination of Hilbert-Schmidt (and other–Bures, monotone) separability and PPT-probabilities [24, 31, 32] (and references therein), but considerably less so, it would seem, as we have attempted here, to the bound-entangled situation. (Perhaps we can regard the Horodecki-state bound-entangled probability of $\frac{1}{5}$ noted above, as the initial result in this area of research.) But of interest in these respects, is the paper [2], in which there was derived “an explicit analytic estimate for the entanglement of a large class of bipartite quantum states, which extends into bound entanglement regions”.

As to the full 35-dimensional set of two-qutrit states itself, evidence has been presented indicating that the associated Hilbert-Schmidt PPT-probability—on the order of 0.0001027 [24, Fig. 9]—is constant over the Casimir invariants of their qutrit subsystems [33, sec.III.A]. (Also, a “repulsion” effect for the Casimir invariants has been observed in the two-qubit case, where the invariants are the Bloch radii of the individual qubits [34]. The two-qutrit case was also examined there.)

In an auxiliary full 63-dimensional 2×4 qubit-qudit analysis, based on 1,200 million iterations, use of the realignment criterion [22] yielded an estimate of 0.00023410917 for the bound-entangled probability and 0.94234319 (conjecturally, $\frac{589}{625} = \frac{17 \cdot 31}{5^4} \approx 0.94234616$) for the entanglement probability, in general. In that (quasirandom Hilbert-Schmidt) analysis, we were not able to detect any finite probability at all of genuinely tripartite entanglement using the Greenberger-Horne-Zeilinger test set out in Example 3 in [10]. (However, in a parallel full 80-dimensional two-qutrit study, the realignment test for entanglement was not passed by any randomly generated states (cf.[12]).)

As a final remark, let us conjecture that the “nonsmooth/jagged” nature of the boundaries of regions of bound entanglement reported above (Figs 3, 14, 22, 23 and 26), will, in some sense—remaining to be made precise—diminishes with increasing dimensions of, say, bipartite systems (cf. [35]).

VII. COMPLIANCE WITH ETHICAL STANDARDS

The author asserts that he has no conflicts of interest or potential such conflicts. The research reported did not involve human participants and/or animals.

Appendix A: Generalized Horodecki-Werner States

1. Two-qutrit case

Let us consider the states that are composed of equally-weighted two-qutrit generalized Horodecki ones (in the sense discussed [sec. IV A]) and the fully mixed two-qutrit state.

Then the PPT-probability for this set is

$$\frac{1}{81} \left(-66 + 21\sqrt{17} + 50\sqrt{3} \sin^{-1} \left(\frac{1}{50} \sqrt{\frac{3}{2} (417 - 7\sqrt{17})} \right) \right) \approx 0.792568. \quad (\text{A1})$$

The entanglement probability for either Jafarizadeh-Behzadi-Akbari (JBA) witness \mathcal{W}_α or \mathcal{W}'_α is given by

$$\begin{cases} \frac{(7-15\alpha)^2}{162(1-3\alpha)^2} & 15\alpha > 7 \vee \alpha < 0 \\ \frac{3\alpha(411\alpha-254)+113}{162(1-3\alpha)^2} & 0 < \alpha \leq \frac{1}{6} \\ \frac{(11-39\alpha)^2}{162(1-3\alpha)^2} & \frac{1}{6} < \alpha < \frac{11}{39} \end{cases}. \quad (\text{A2})$$

The bound-entangled probability for either witness is

$$\frac{3\alpha(411\alpha - 254) + 113}{162(1 - 3\alpha)^2}, \quad (\text{A3})$$

for $\alpha \in [\frac{1}{309} (71 - 6\sqrt{17}) \approx 0.149713, \frac{1}{6}]$ and

$$\frac{(11 - 39\alpha)^2}{162(1 - 3\alpha)^2}, \quad (\text{A4})$$

for $\alpha \in [\frac{1}{6}, \frac{11}{39}]$. (In these last two intervals, all the entanglement probability is bound—as can be seen from (A2).)

2. Two-ququart case

Now, for the class of equally-weighted generalized Horodecki two-ququart states (in the above JBA sense again [sec. IV B]) and the fully mixed two-ququart state, the PPT-probability

Entanglement probabilities

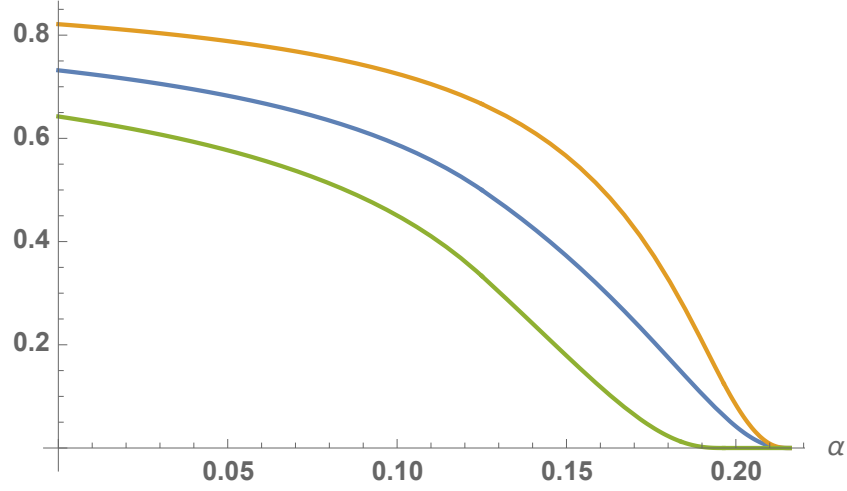


FIG. 31: The equally-weighted (Horodecki-Werner) two-ququart entanglement probability function (A6) for either JBA witness \mathcal{W}_α or \mathcal{W}'_α , along with the dominant union and subordinate intersection curves, obtained by application of the two witnesses. The interval employed is $\alpha \in [0, \frac{19}{88}]$.

is

$$\frac{437}{192} - \frac{7\sqrt{7}}{12} \approx 0.732687. \quad (\text{A5})$$

The entanglement probability for either JBA witness is

$$\begin{cases} \frac{(40\alpha-13)^3}{8192(4\alpha-1)^3} & \alpha > \frac{13}{40} \vee \alpha < 0 \\ \frac{(88\alpha-19)^3}{8192(4\alpha-1)^3} & \frac{1}{8} < \alpha < \frac{19}{88} \\ \frac{460288\alpha^3 - 330816\alpha^2 + 78024\alpha - 5995}{8192(4\alpha-1)^3} & 0 < \alpha < \frac{1}{8} \end{cases}. \quad (\text{A6})$$

In Fig. 31, we show this function over the interval $\alpha \in [\frac{1}{8}, \frac{19}{88}]$ along with the entanglement probabilities based on the union and intersection of application of the two witnesses. In a somewhat indirect fashion, We have been able to establish—through examination of numerous specific values of α and certain auxiliary analyses—that the bound-entangled probability function for either witness takes the form (Fig. 32)

$$\frac{8\alpha(8\alpha(14600\alpha - 9537) + 16599) - 9623}{12288(4\alpha - 1)^3}, \quad (\text{A7})$$

over $\alpha \in [1/872(161 - 18\sqrt{7}) \approx 0.130019, \frac{11}{56} \approx 0.196429]$. The nature of the function outside this interval remains under examination.

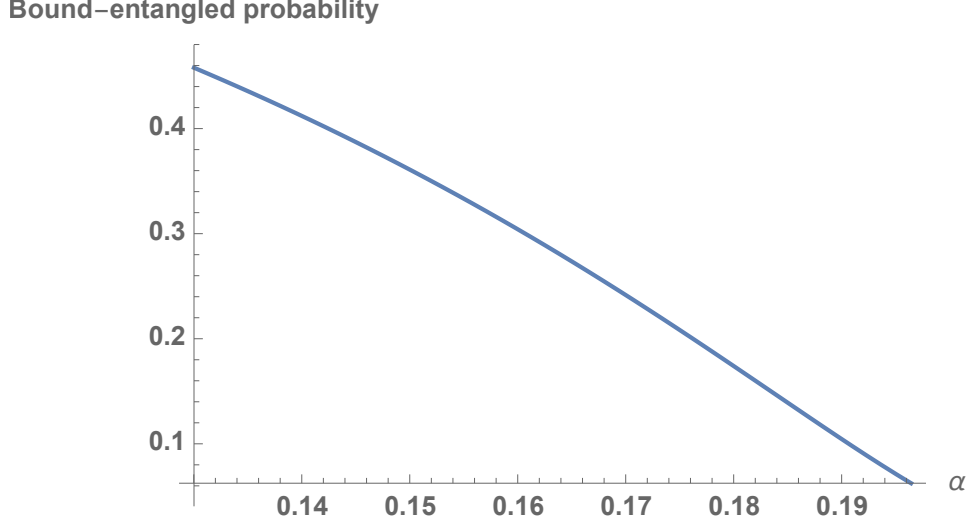


FIG. 32: Bound-entangled probability function (A7) for the equally-weighted Horodecki-Werner two-quart scenario—restricted to the interval $\alpha \in [1/872(161 - 18\sqrt{7}) \approx 0.130019, \frac{11}{56} \approx 0.196429]$.

3. Two-ququints

The entanglement probability for this still higher-dimensional equally-weighted case for either \mathcal{W}_α or \mathcal{W}'_α is

$$\begin{cases} \frac{(85\alpha-21)^4}{781250(5\alpha-1)^4} & \alpha > \frac{21}{85} \vee \alpha < 0 \\ \frac{(165\alpha-29)^4}{781250(5\alpha-1)^4} & \frac{1}{10} < \alpha < \frac{29}{165} \\ \frac{436080625\alpha^4 - 339038500\alpha^3 + 98070150\alpha^2 - 12476260\alpha + 586769}{781250(5\alpha-1)^4} & 0 < \alpha \leq \frac{1}{10} \end{cases} \quad (\text{A8})$$

The PPT-probability is ≈ 0.758301 . At $\frac{1}{6}$, the bound-entangled probability is, interestingly, $\frac{6561}{781250} = \frac{3^8}{2 \cdot 5^8} \approx 0.00839808$. It jumps at $\alpha = \frac{1}{7}$ to $0.1646314041874492 = 0.0119320240085435 + \frac{8}{625} + \frac{2008781 - 157760\sqrt{145}}{1953125} + \frac{72(696\sqrt{145} - 7925)}{390625}$.

In Fig. 33, we show a numerically-derived plot of this function over $\alpha \in [0, \frac{1}{6}]$.

An important question that remains is whether outside the intervals employed by Jarafizadeh, Behzadi, and Akbari, \mathcal{W}_α and \mathcal{W}'_α can serve as entanglement witnesses—and, thus, whether a number of probabilities presented above in this section that were termed “entanglement” and “bound-entangled” are, in fact, so.

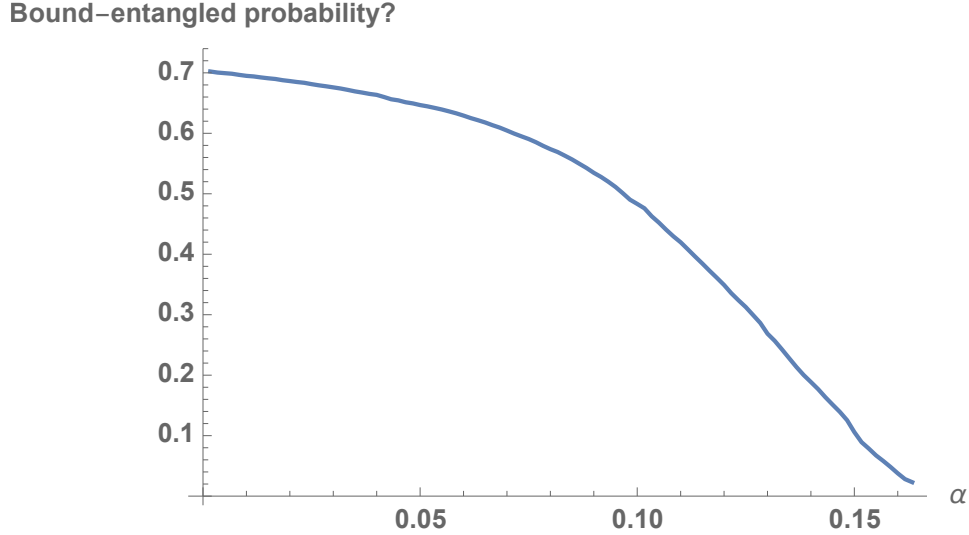


FIG. 33: Numerically-derived plot for equally-weighted two-quint scenario over $\alpha \in [0, \frac{1}{6}]$.

Acknowledgments

This research was supported by the National Science Foundation under Grant No. NSF PHY-1748958. Nicolas Tessore greatly assisted in the carrying out of many of the calculations reported above. I also strongly thank Dariuz Chruściński for sharing his entanglement-witness expertise.

-
- [1] K. Życzkowski, P. Horodecki, A. Sanpera, and M. Lewenstein, *Physical Review A* **58**, 883 (1998).
 - [2] J. Bae, M. Tiersch, S. Sauer, F. de Melo, F. Mintert, B. Hiesmayr, and A. Buchleitner, *Physical Review A* **80**, 022317 (2009).
 - [3] B. Baumgartner, B. C. Hiesmayr, and H. Narnhofer, *Physical Review A* **74**, 032327 (2006).
 - [4] B. Baumgartner, B. C. Hiesmayr, and H. Narnhofer, *Physics Letters A* **372**, 2190 (2008).
 - [5] L. Derkacz and L. Jakóbczyk, arXiv preprint arXiv:0707.1575 (2007).
 - [6] G. Sentís, J. N. Greiner, J. Shang, J. Siewert, and M. Kleinmann, arXiv preprint arXiv:1804.07562 (2018).
 - [7] D. Chruściński and A. Rutkowski, *Physics Letters A* **375**, 2793 (2011).
 - [8] M. Jafarizadeh, N. Behzadi, and Y. Akbari, *The European Physical Journal D* **55**, 197 (2009).

- [9] B. C. Hiesmayr and W. Löffler, *New journal of physics* **15**, 083036 (2013).
- [10] J. Bae, D. Chruściński, and B. C. Hiesmayr, arXiv preprint arXiv:1811.09896 (2018).
- [11] *Construct, in some manner, a four-dimensional regionplot*,
URL <https://mathematica.stackexchange.com/questions/202195/construct-in-some-manner-a-four-dimensional-regionplot>.
- [12] A. Gabdulin and A. Mandilara, arXiv preprint arXiv:1906.08963 (2019).
- [13] J. DiGuglielmo, A. Sambrowski, B. Hage, C. Pineda, J. Eisert, and R. Schnabel, *Physical review letters* **107**, 240503 (2011).
- [14] D. Chruściński, G. Sarbicki, and F. Wudarski, *Physical Review A* **97**, 032318 (2018).
- [15] K.-C. Ha and S.-H. Kye, *Physical Review A* **84**, 024302 (2011).
- [16] D. Chruściński and F. A. Wudarski, *Open Systems & Information Dynamics* **18**, 375 (2011).
- [17] *Can a certain series of integrals over $[0, \frac{1}{16}]$ be solved using integration-by-parts?*,
URL <https://math.stackexchange.com/questions/3228259/can-a-certain-series-of-integrals-over-0-frac116-be-solved-using-integr>.
- [18] D. Chruściński and F. A. Wudarski, *Open Systems & Information Dynamics* **19**, 1250020 (2012).
- [19] D. Chruściński and F. A. Wudarski, arXiv preprint arXiv:1204.5283 (2012).
- [20] D. Chruściński, *Journal of Physics A: Mathematical and Theoretical* **47**, 424033 (2014).
- [21] D. Chruściński and G. Sarbicki, *Journal of Physics A: Mathematical and Theoretical* **47**, 483001 (2014).
- [22] K. Chen and L.-A. Wu, arXiv preprint quant-ph/0205017 (2002).
- [23] J. Shang, A. Asadian, H. Zhu, and O. Gühne, *Physical Review A* **98**, 022309 (2018).
- [24] P. B. Slater, arXiv preprint arXiv:1901.09889 (2019).
- [25] *How can one generate an open ended sequence of low discrepancy points in 3d?*,
URL <https://math.stackexchange.com/questions/2231391/how-can-one-generate-an-open-ended-sequence-of-low-discrepancy-points-in-3d>.
- [26] *The unreasonable effectiveness of quasirandom sequences*, URL <http://extremelearning.com.au/unreasonable-effectiveness-of-quasirandom-sequences/>.
- [27] A. R. Rau, *Quantum Information Processing* **17**, 1 (2018), ISSN 1570-0755, URL <https://doi.org/10.1007/s11128-018-1985-8>.
- [28] C. F. Dunkl and P. B. Slater, *Random Matrices: Theory and Applications* **4**, 1550018 (2015).

- [29] K. Życzkowski, Physical Review A **60**, 3496 (1999).
- [30] Y. Zhou, J. Yu, Z. Yan, X. Jia, J. Zhang, C. Xie, and K. Peng, Physical review letters **121**, 150502 (2018).
- [31] P. B. Slater, Quantum Information Processing **17**, 83 (2018).
- [32] P. B. Slater, arXiv preprint arXiv:1809.09040 (2018).
- [33] P. B. Slater, Quantum Information Processing **15**, 3745 (2016).
- [34] P. B. Slater, International Journal of Quantum Information **14**, 1650042 (2016).
- [35] S. Beigi and P. W. Shor, Journal of Mathematical Physics **51**, 042202 (2010).